Science of the Total Environment 958 (2025) 177869

Contents lists available at ScienceDirect

Science of the Total Environment

journal homepage: www.elsevier.com/locate/scitotenv

Comparing statistical and deep learning approaches for simultaneous prediction of stand-level above- and belowground biomass in tropical forests

Bao Huy [a,b,*], Krishna P. Poudel [c], Hailemariam Temesgen [b], Christian Salas-Eljatib [d], Nguyen Quy Truong [a], Nguyen Quy Khiem [a]

[a] Forest Resources and Environment Management Consultancy (FREM), 06 Nguyen Hong, Buon Ma Thuot, Dak Lak 630000, Viet Nam
[b] Department of Forest Engineering, Resources and Management, Oregon State University (OSU), Corvallis, OR 97333, USA
[c] Department of Forestry, Mississippi State University, P.O. Box 9681, Mississippi State, MS 39762, USA
[d] Departamento de Gestión Forestal y su Medio Ambiente, Universidad de Chile, Santiago, Chile

HIGHLIGHTS

- Innovative developed DLAMs for simultaneously predicting stand-level *AGB* and *BGB*.
- DLAMs substantially enhanced the reliability of simultaneously predicting *AGB* and *BGB*.
- DLAMs are recognized as the optimal approach compared to WNSUR and MARS methods.
- A well-designed multi-output deep neural network is key to finding the best DLAMs.

GRAPHICAL ABSTRACT

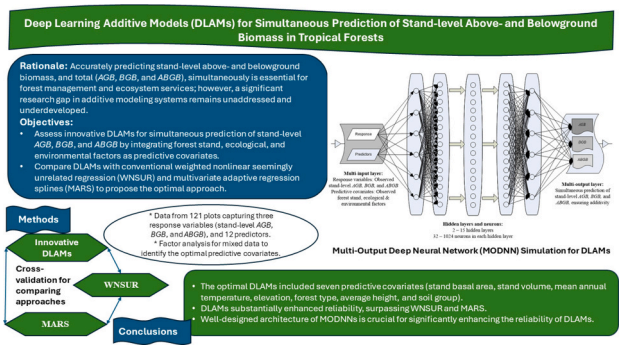

ARTICLE INFO

Editor: Kuishuang Feng

Keywords:
Deep learning
Forest carbon
Simultaneous additive models
Tropical forest

ABSTRACT

Accurate and cost-effective prediction of aboveground biomass (*AGB*), belowground biomass (*BGB*), and the total (*ABGB*) at stand-level within tropical forests is crucial for effective forest ecological management and the provision of forest ecosystem services. Although there has been research on simultaneously fitting biomass equations for tree components, rather few studies focus on simultaneously predicting *AGB* and *BGB* at stand-level while maintaining additivity. We developed innovative Deep Learning Additive Models (DLAMs) for the simultaneous predictions of stand-level *AGB*, *BGB*, and *ABGB* integrating forest stand, ecological, and environmental factors as predictive covariates and compared them with conventional weighted nonlinear seemingly unrelated regression (WNSUR) and multivariate adaptive regression splines (MARS). Data for this study were collected from 121 plots distributed in two tropical forest types (dipterocarp and evergreen broadleaf) across five ecological regions of Vietnam, capturing three response variables (*AGB*, *BGB*, and *ABGB*), and 12 predictors. Factor analysis for mixed data was employed to identify the optimal covariates. Cross-validation results demonstrated that DLAMs

* Corresponding author at: Forest Resources and Environment Management Consultancy (FREM), 06 Nguyen Hong, Buon Ma Thuot, Dak Lak 630000, Viet Nam.
E-mail addresses: BaoHuy.frem@gmail.com (B. Huy), Krishna.Poudel@msstate.edu (K.P. Poudel), Temesgen.Hailemariam@oregonstate.edu (H. Temesgen), Christian.Salas@uchile.cl (C. Salas-Eljatib), QuyTruong.Ng@gmail.com (N.Q. Truong), QuyKhiem.frem@gmail.com (N.Q. Khiem).

https://doi.org/10.1016/j.scitotenv.2024.177869
Received 24 August 2024; Received in revised form 8 November 2024; Accepted 29 November 2024
Available online 5 December 2024

substantially enhanced the reliability of simultaneous predictions of forest biomass components compared to the conventional WNSUR and MARS methods. The optimal DLAMs included seven predictive covariates (stand basal area (*G*), stand volume (*V*), mean annual temperature (*T*), elevation (*EL*), forest type (*FT*), average height (*Hg*), and soil group (*SG*)). They had mean absolute percent errors (MAPEs) of 6.3 %, 4.3 %, and 5.3 % for the simultaneous prediction of *AGB*, *BGB*, and *ABGB*, respectively. The MAPEs for the DLAMs approach were substantially lower than those for the WNSUR alternative by 2.9 %, 14.0 %, and 2.4 %, and lower than those for the MARS method by 4.3 %, 11.6 %, and 4.1 % for predicting *AGB*, *BGB*, and *ABGB* simultaneously, respectively. Conducting experiments in designing multi-input multi-output deep neural networks was essential for significantly improving the reliability of the simultaneous predictions from the DLAMs.

1. Introduction

Forest biomass offers important ecosystem services, including maintaining a stable environment, ecosystem, and climate (Pravalie et al. 2023). While the aboveground biomass carbon pool is the central and most prominent carbon reservoir within the tropical forest ecosystem, the belowground biomass carbon pool plays a crucial role in the carbon cycle by facilitating the transfer and storage of carbon within the soil (Vashum and Jayakumar 2012). Therefore, accurately and simultaneously estimating stand-level above- and belowground biomass, including their total (*AGB*, *BGB*, and *ABGB* = *AGB* + *BGB*, respectively), while minimizing resource requirements, is paramount for

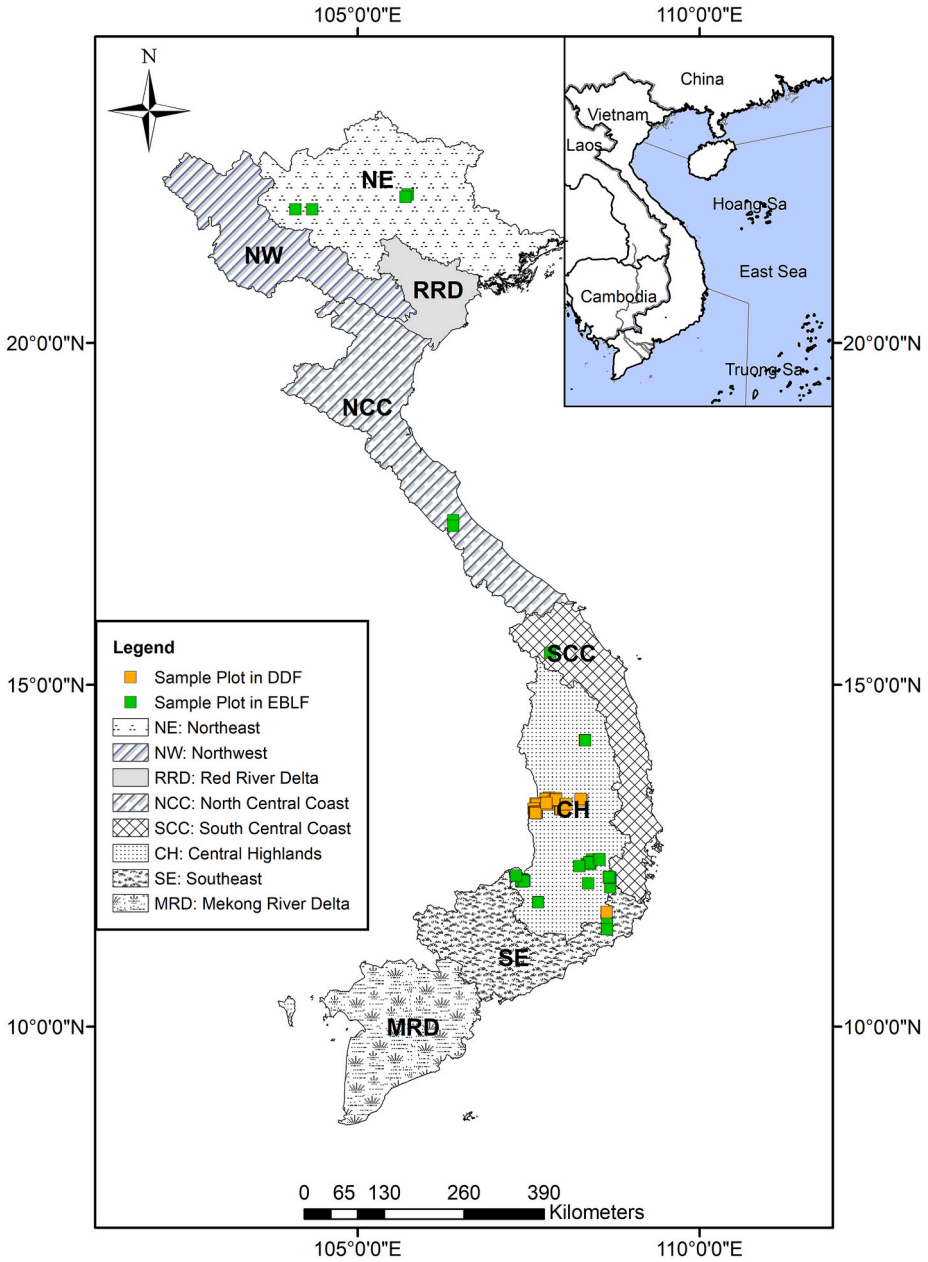

Fig. 1. Spatial distribution of sample plots in Dry Dipterocarp Forest (DDF) and Evergreen Broadleaf Forest (EBLF) across five ecoregions of Vietnam.

effective forest ecological management. Moreover, it has significant implications for carbon credit programs such as Reducing Emissions from Deforestation and Forest Degradation (REDD+) (Calderon-Balcazar et al. 2023) and initiatives promoting forest environmental services such as Carbon Payment for Forest Environmental Services (C-PFES) (USAID 2018). Therefore, there is a need for the development, cross-validation and comparison of additive models – encompassing statistical approaches and leveraging advanced deep learning (DL) technology in artificial intelligence (AI) – to identify the optimal modeling system for directly forecasting forest biomass carbon pools simultaneously at the stand-level of tropical forests. This approach saves time and costs compared to tree biomass additive models (Kralicek et al. 2017; Huy et al. 2024).

Forest biomass estimation relies on allometric equations that predict tree-level above- and belowground biomass (*agb* and *bgb*, respectively) (Vashum and Jayakumar 2012), based on commonly predictive covariates such as diameter at breast height (*d*), tree height (*h*) and wood density (*wd*), which are subsequently used to convert estimated tree biomass into biomass carbon stocks in above- and belowground components in tropical mixed species forests (IPCC 2003, 2006; Poudel and Temesgen 2016; Kralicek et al. 2017; Huy et al. 2016a, 2016b). This requires precise tree species identification to determine the *wd* values for each species. Identifying tree species in tropical mixed-species forests requires expertise in forest botany; without such experts, the reliability of the data may be compromised. This can incur significant costs in resources, including time, budget, and professional labor.

Additivity of component masses is one of the desired properties in developing biomass models, which is often ensured by fitting component models as a system with weighted nonlinear seemingly unrelated regression (WNSUR) (Parresol 2001; Huy et al. 2023; Xin et al. 2023). Multivariate adaptive regression splines (MARS) is an algorithm designed for non-parametric regression to address complex linear and nonlinear regression problems (Friedman 1991). MARS is specifically designed to capture additive and interaction effects (Koc and Bozdogan 2015) and offers a flexible approach to regression modeling in high-dimensional datasets (Huang et al. 2019; Milborrow 2021; Yasmirullah et al. 2021). This makes MARS an attractive option for simultaneously modeling stand-level *AGB*, *BGB*, and total, but limited studies have applied MARS in this particular context. Only a few researchers have successfully employed MARS in combination with remote sensing techniques to estimate forest height and total *AGB* (Filippi et al. 2014; Laurin et al. 2016; Arjasakusuma et al. 2020) or to predict forest growth and yield (Lei 2019).

Machine learning (ML) approaches have been widely applied in recent years. In terms of forestry research, He et al. (2023) developed ML techniques to estimate stand-level biomass in mixed forests in northeast China, while Xu et al. (2022) employed ML techniques and multi-task artificial neural networks (ANNs) to estimate biomass for multiple tree components simultaneously. DL — a subset of ML, can facilitate the exploratory analysis of relationships among forest ecological and environmental factors (Wang et al. 2021; Ozdemir et al. 2022). DL algorithms have also been developed to model the height-diameter relationship in complex tropical rainforest ecosystems (Ogana and Ercanli 2021) and to predict tree crown width in natural mixed forests (Qin et al. 2023). Recently, Huy et al. (2022b, 2024) developed single-output DL models to predict tree *AGB* and multi-output DL models for simultaneous predictions of tree-level above- and belowground biomass in tropical forests.

The literature on modeling stand-level forest biomass is limited (Xin et al. 2023). There is a need to develop and select optimal, parsimonious stand-level biomass models capable of directly and simultaneously predicting *AGB*, *BGB*, and their total *ABGB*. Such models have the potential to substantially improve accuracy, reduce costs, and minimize professional labor by eliminating the necessity to identify individual tree species or species-specific *wd* predictive variables compared to using tree-level additive biomass equations in tropical mixed- species forests.

Table 1
Statistical metrics of responses and predictive covariates.

ID	Variables	Min.	Mean	Max.	Std.
Responses					
1	*AGB* (Mg ha^{-1})	10.4	200.7	1012.1	206.1
2	*BGB* (Mg ha^{-1})	1.8	24.0	84.3	17.6
3	*ABGB* (Mg ha^{-1})	12.2	224.6	1080.9	222.9
Predictive covariates					
	Forest stand variables				
4	*Dg* (cm)	8.5	19.2	32.3	4.7
5	*Hg* (m)	4.7	12.3	20.7	3.8
6	*N* (tree ha^{-1}; with d $\geq$ 5 cm)	156	847	2760	462
7	*G* (m^2 ha^{-1})	3.8	25.7	92.6	18.8
8	*V* (m^3 ha^{-1})	9.1	220.5	1043.8	221.9
9	*FT* (categorical variable)	DDF, EBLF			
	Ecological factors				
10	*EC* (categorical variable)	CH, NCC, NE, SCC, SE			
11	*SG* (categorical variable)	FA, OA, RF			
12	*P* (mm year^{-1} averaged)	1070	1880	2216	225
13	*T* (°C year^{-1} averaged)	15.4	22.9	26.3	3.3
14	*EL* (m)	156	613	1870	479
15	*SL* (degree)	0	9	50	12

Note: *AGB*: aboveground biomass, *BGB*: belowground biomass, *ABGB*: above- and below-ground biomass at stand-level. *Dg*: quadratic mean diameter at breast height (*d*), *Hg*: average tree height corresponding to *Dg*, *N*: number of trees per hectare, *G*: stand basal area per hectare, *V*: stand volume per hectare. *FT*: Forest type, DDF: Dry Dipterocarp Forest, EBLF: Evergreen Broadleaf Forest. *EC*: ecoregion, CH: Central Highlands, NCC: North Central Coast, NE: northeast, SCC: South Central Coast, SE: southeast. *SG*: soil group, FA: Ferric Acrisols, OA: Orthic Acrisols, RF: Rhodic Ferrasols. *P*: mean annual precipitation, *T*: mean annual temperature. *EL*: elevation. SL: slope. Statistical metrics were calculated based on 121 sample plots. For *FT*: 61 plots for DDF and 60 plots for EBLF. For *EC*: 110 plots for CH, 2 plots for NCC, 4 plots for NE, 2 plots for SCC, and 3 plots for SE. For *SG*: 61 plots for FA, 39 plots for OA and 21 plots for RF.

The objectives of this study were to 1) Assess deep learning additive models (DLAMs) for simultaneously predicting *AGB*, *BGB*, and *ABGB* at the stand-level integrating forest stand, ecological, and environmental factors as predictive covariates in tropical mixed-species forests, and 2) Perform cross-validations to assess the reliability and accuracy of the statistical methods WNSUR and MARS, along with DLAMs, to propose the optimal approach for the simultaneous prediction of *AGB*, *BGB*, and *ABGB* at the stand-level, ensuring additivity. We hypothesized that innovative DLAMs can substantially enhance the accuracy of stand-level *AGB*, *BGB*, and total *ABGB* predictions in tropical mixed- species forests compared to conventional statistical approaches.

2. Materials and methods

2.1. Studied ecoregions

This study was carried out in five out of eight ecological regions of Vietnam, namely the Central Highlands (CH), the North Central Coast (NCC), the Northeast (NE), the South Central Coast (SCC), and the Southeast (SE) (Fig. 1). We studied two types of forests: Dry Dipterocarp Forest (DDF) and Evergreen Broadleaf Forest (EBLF). EBLF was studied in all five ecoregions, while DDF was only studied in the two where it is distributed, CH and SE. The characteristics and variations in the forest stand and the ecology and environment of the study areas are presented in Table 1.

2.2. Data and selection of variables

A total of 121 purposive sample plots were performed, ranging in size from 500 to 10,000 m^2, with the predominant plot size being 900 m^2, with 61 plots designated for DDF and 60 plots for EBLF. The sample plots were distributed across various forests, ranging from immature to mature or heavily to lightly disturbed. Consequently, smaller plots were

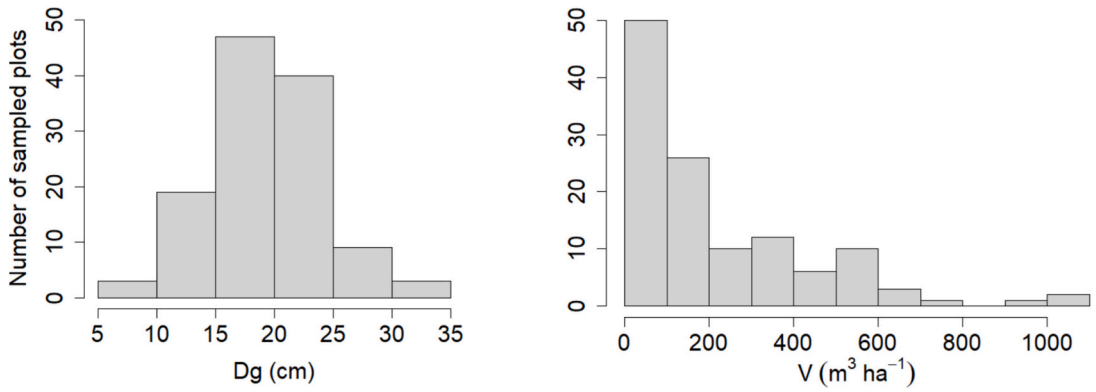

Fig. 2. Distribution of sample plots by quadratic mean diameter at breast height (*Dg*) in classes (left) and by classes of stand volume (*V*) (right).

Table 2
Individual tree *agb* and *bgb* equations used for estimating stand-level above- and belowground biomass in two tropical forest types and across five ecoregions.

Forest types	Ecoregions	Tree allometric equations	Sources of equations
DDF	CH, SE	$agb = 0.0620 \times d^{2.264} \times h^{0.5142} \times wd^{0.7946}$	Huy et al. (2016b)
		$bgb = 56.48 \times (d^2h)^{0.9132}$	Kralicek et al. (2017)
EBLF	CH	$agb = 0.7988 \times (d^2hwd)^{0.9656}$	Huy et al. (2016a)
	NCC	$agb = 0.6805 \times (d^2hwd)^{0.9385}$	Huy et al. (2016a)
	NE	$agb = 0.6801 \times (d^2hwd)^{0.9384}$	Huy et al. (2016a)
	SCC	$agb = 0.6852 \times (d^2hwd)^{0.9395}$	Huy et al. (2016a)
	SE	$agb = 0.6473 \times (d^2hwd)^{0.9309}$	Huy et al. (2016a)
	All	$bgb = 0.1689 \times d^{1.765}$	Kralicek et al. (2017)

Note: *agb*: tree aboveground biomass (kg tree^{-1}), *bgb*: tree belowground biomass (kg tree^{-1}). *d*: diameter at breast height (cm), *h*: tree height (m), *wd*: wood density (g cm^{-3}). d^2h is a surrogate of volume in m^3 = $(d/100)^2 \times h$ and d^2hwd is a surrogate of biomass in kg = $d^2h \times wd \times 1000$. Forest type: DDF: Dry Dipterocarp Forest, EBLF: Evergreen Broadleaf Forest. Ecoregion: CH: Central Highlands, NCC: North Central Coast, NE: northeast, SCC: South Central Coast, SE: southeast.

located in high-density regenerating forest areas, while larger plots were placed in mature or heavily disturbed forests with sparse density. The distribution of sample plots based on quadratic mean diameter at breast height (*Dg*) follows a bell-shaped curve, while the distribution of stand volume exhibits a reverse J-shaped curve (Fig. 2). This indicates that tropical forests in Vietnam are concentrated at volumes below 200 m^3 ha^{-1}, with a marked decrease in forest distribution as volume exceeds 200 m^3 ha^{-1}.

For each sample plot, the coordinates were determined, and the tree variables *d* and *h* were measured for all of the trees. We measured all individuals with *d* larger or equal to 5 cm. The species name of the trees was also identified. Additionally, ecological environmental factors were assessed and recorded in each sample plot.

2.2.1. Response variables

The study considered three simultaneous response variables: *AGB*, *BGB* and total *ABGB* at stand-level. These values were derived by applying tree-level biomass models such as the equations of tree aboveground biomass (*agb*) and tree belowground biomass (*bgb*) developed by Huy et al. (2016a, 2016b) and Kralicek et al. (2017) for two forest types, DDF and EBLF, across ecoregions of CH, NCC, NE, SCC and SE. For the DDF, the tree *agb* equation incorporates three tree predictors: *d*, *h* and *wd*; on the other hand, the tree *bgb* equation relies on the common tree predictors *d* and *h*; and these tree *agb* and *bgb* equations were applied in both ecological regions of CH and SE, where DDF is distributed. In the case of EBLF, the tree *agb* model is specific to each of the five ecoregions CH, NCC, NE, SCC and SE and utilizes a combination of three tree predictors *d*, *h*, and *wd*. In comparison, the tree *bgb* model is shared among all five ecoregions and only uses the tree predictor *d*. The tree *agb* and *bgb* models used in the study can be found in Table 2. When calculating tree *agb* using equations that incorporate the predictive variable *wd*, which were determined based on species-specific data from databases published by Zanne et al. (2009), Huy et al. (2016a, 2016b), and Kralicek et al. (2017). After obtaining the calculated *agb* and *bgb* values for each tree within each sample plot, stand-level *AGB* represented the sum of tree *agb* and stand-level *BGB* represented the sum of tree *bgb* within the plot. Furthermore, the stand-level *ABGB* in the plot was calculated as the sum of *AGB* and *BGB*. *AGB*, *BGB*, and *ABGB* values were then converted to Mg per hectare for each plot.

2.2.2. Predictive covariates

This study consisted of 12 predictors, which are as follows: The forest stand included six variables calculated at the plot level and expressed per hectare (ha). These variables included *Dg*, average height (*Hg*) corresponding to *Dg* obtained from the *h-d* regression model (Huy et al. 2022a), stand density (*N*), stand basal area (*G*), stand volume (*V*) calculated as the sum of the volumes of individual trees based on their *d*, *h* and a form factor value of 0.45 (Vanclay 1994), and a categorical variable representing the forest type (*FT*) including DDF and EBLF. The ecological and environmental variables comprised six factors recorded or extracted at the plot coordinates. These variables included climate variables such as mean annual temperature (*T*) and mean annual precipitation (*P*) averaged over 30 years (1970–2000), obtained from raster files of the climate surface with a spatial resolution of 30 s (~1 km) (Fick and Hijmans 2017); the soil group (*SG*) was categorical into Ferric Acrisols (FA), Orthic Acrisols (OA), and Rhodic Ferrasols (RF) extracted from the soil map of FAO-UNESCO (2005); the ecoregion (*EC*) variable encompassed five categories: CH, NCC, NE, SCC and SE, and elevation (*EL*) and slope (*SL*) variables were recorded for each sample plot. These ecological and environmental variables provide additional information on the study area's climate, soil, ecoregion, and topography, potentially influencing tropical forest biomass dynamics.

A summary of the response variables and predictive covariates is shown in Table 1.

2.2.3. Selection of predictive covariates

Factor analysis for mixed data (FAMD) (Huy et al. 2022b) was employed to identify and select the most influential predictive covariates for stand-level *AGB*, *BGB*, and *ABGB*. This statistical technique allows for the analysis of both numeric and categorical variables simultaneously, enabling a comprehensive assessment of the impact of the covariates on stand-level biomass variables. In the study, 15 variables were considered, comprising 3 response numeric variables (*AGB*, *BGB*, and *ABGB*) and 12 predictive covariates. The predictive variables consisted of 9 numeric variables (*Dg*, *Hg*, *N*, *G*, *V*, *T*, *P*, *EL*, and *SL*) and 3

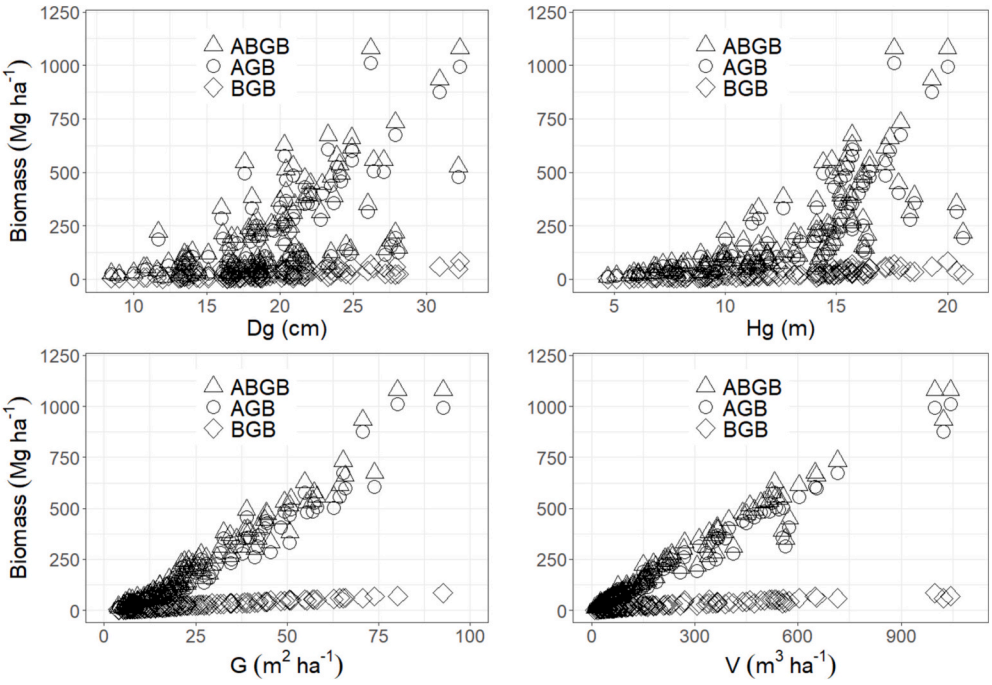

Fig. 3. Scatter plots stand-level above- and belowground biomass and their total (*AGB*, *BGB* and *ABGB*, respectively) versus stand covariates of quadratic mean diameter at breast height (*Dg*), average tree height (*Hg*) corresponding to *Dg*, stand basal area (*G*) and stand volume (*V*).

nominal categorical variables (*FT*, *SG*, and *EC*). The factor analysis was performed using the FAMD function in the FactoMineR package (Lê et al. 2008) implemented in R (R Core Team 2023).

2.3. Weighted nonlinear seemingly unrelated regression (WNSUR)

The relationships between stand-level *AGB*, *BGB*, and total *ABGB* responses to the stand variables follow a power function and exhibit heterogeneity of errors (Fig. 3) and additivity. Therefore, the WNSUR method needs to be applied (Parresol 2001; Poudel and Temesgen 2016; Kralicek et al. 2017; Huy et al. 2019, 2023; Xin et al. 2023).

To select the model form for each component – stand-level *AGB*, *BGB*, and *ABGB* – based on stand covariates (Xin et al. 2023), we used weighted nonlinear fitting by maximum likelihood (WNML) by applying the 'nlme' function (Lindstrom and Bates 1990) on the independent component models in the statistical software R (R Core Team 2023).

This study also examined a WNSUR modeling system that simultaneously predicts stand-level *AGB*, *BGB*, and *ABGB* by incorporating environmental and ecological factors. In this case, the biomass models take the form of two parts: a selected average biomass model and a modifier. The general model form is (Huy et al. 2022a, 2022b) as follows:

$$\text{Biomass Component}_i = \text{Average}_i \times \text{Modifier}_i + \varepsilon_i \quad (1)$$

where Average_i is the i^{th} independent model of *AGB/BGB* versus the stand variables selected by cross-validation; Modifier_i is the i^{th} exponential function that adjusts the predicted values of the biomass component i based on the selected environmental and ecological variables from FAMD. ε_i is the random error of the i^{th} function.

The detailed form of the modeling system (Eq. 1) for simultaneously predicting stand-level *AGB*, *BGB*, and *ABGB* associated with environmental and ecological variables fitted by WNSUR is expressed as follows (Huy et al. 2022a):

$$AGB = a_1 X_{1j}^{b1j} \prod_{k=1}^{n} exp(e_{1k}(\text{factor}_k – \text{averaged value of factor}_k)) + \varepsilon_1 \quad (2)$$

$$BGB = a_2 X_{2j}^{b2j} \prod_{k=1}^{n} exp(e_{2k}(\text{factor}_k – \text{averaged value of factor}_k)) + \varepsilon_2 \quad (3)$$

$$\begin{aligned} ABGB =& AGB + BGB \\ =& a_1 X_{1j}^{b1j} \prod_{k=1}^{n} exp(e_{1k}(\text{factor}_k – \text{averaged value of factor}_k)) \\ &+ a_2 X_{1j}^{b1j} \prod_{k=1}^{n} exp(e_{2k}(\text{factor}_k – \text{averaged value of factor}_k)) + \varepsilon_3 \end{aligned} \quad (4)$$

where $\text{Average}_i = a_i X_{ij}^{bij}$ functions selected from cross-validation of independent models fitted by WNML for stand-level *AGB* and *BGB* versus stand variables; a_i and b_{ij} are parameters of the power model i (i = 1, 2, 3 for the *AGB*, *BGB*, and *ABGB*, respectively) and the j^{th} predictor; X_{ij} represents the predictor or combination of stand variables for the i^{th} equation and the j^{th} predictor. $Modifier_i$ represents the ith *Modifier* equation $= \prod_{k=1}^{n} exp(e_{ik} \times (variable_k - averaged\ value\ of\ factor_k))$, where e_{ik} is the parameter for the i^{th} Modifier equation and the k^{th} factor, and n is the number of environmental and ecological covariates selected based on FAMD; the averaged values of factor_k are presented in Table 1; for categorical factors, encoding was performed as follows: *FT*: DDF = 1 and EBLF = 2, with a mean value of 1.5; *SG*: FA, OA, and RF were encoded as 1, 2 and 3, respectively, with a mean value of 1.7. In the Modifier function, when factor values are equal to their means, the Modifier value is 1 and the Biomass Component equation is equal to the Average function (Huy et al. 2022a). However, when environmental and ecological factors deviate from their means, the biomass component models are adjusted according to the exponential function and the parameters. ε_i is the residual for the i^{th} equation (i = 1, 2, 3). Weight variable $= 1/X_j^{\delta}$, δ: the variance function coefficient.

The WNSUR models associated with environmental and ecological covariates (Eqs. (2), (3), (4)) were performed using the generalized least squares (GLS) method in SAS software (SAS Institute Inc. 2014).

2.4. Multivariate Adaptive Regression Spline (MARS)

The MARS model is formulated using an expansion in product spline basis functions. Importantly, the data automatically determines the number of basis/hinge functions and the coefficients linked to each product degree and knot (Friedman 1991). The general MARS forms (Friedman and Silverman 1989; Friedman 1991; Huang et al. 2019) for simultaneously predicting responses are as follows:

$$AGB = a_1 + \sum_{h=1}^{k} b_{1h} \bullet h(X_{zh} - c_{zh}, c_{zh} - X_{zh}) + \varepsilon_1 \quad (5)$$

$$BGB = a_2 + \sum_{h=1}^{k} b_{2h} \bullet h(X_{zh} - c_{zh}, c_{zh} - X_{zh}) + \varepsilon_2 \quad (6)$$

$$ABGB = a_3 + \sum_{h=1}^{k} b_{3h} \bullet h(X_{zh} - c_{zh}, c_{zh} - X_{zh}) + \varepsilon_3 \quad (7)$$

where *AGB*, *BGB*, and *ABGB* represent the stand-level above- and belowground, and total biomass, respectively; a_i is the intercept term for the i^{th} model ($i = 1$, 2 and 3 for the equations of simultaneous predictions of *AGB*, *BGB* and *ABGB*, respectively); h represents the hinge function with a total of k functions; b_{ih} is the coefficient associated with the model i^{th} for the h^{th} function; X_{zh} is the z^{th} predictive variable chosen in the h^{th} function; c_{zh} is a constant known as a knot value associated with the z^{th} variable for the hth function; ε_i denotes the random error of the i^{th} model. With three *AGB*, *BGB* and *ABGB* responses, MARS builds three simultaneous component models. Each model has the same set of hinge functions '$h(X_{zh} - c_{zh}, c_{zh} - X_{zh})$'; they only differ in the coefficients 'a_i', 'b_{ih}' and random errors 'ε_i' (Milborrow 2021).

The basic/hinge function is a piecewise-linear function that captures nonlinear relationships between responses and predictor variables. Within the hinge function, numerical values act as thresholds or cut-off points, effectively partitioning the input variables in the MARS models. This partitioning enables the modeling of variable interactions and nonlinearities.

This study has three continuous responses (stand-level *AGB*, *BGB*, and *ABGB*) and seven predictors (*G*, *M*, *T*, *EL*, *FT*, *Hg*, and *SG*) selected using FAMD. Among the predictors, two are nominal categorical variables: *FT* and *SG*. Notably, MARS can effectively handle continuous and nominal categorical variables (Friedman 1993; Yasmirullah et al. 2021).

This study employed the 'earth' in R (R Core Team 2023) for MARS modeling (Milborrow 2023) to develop, cross-validate, and select the optimal equation system for simultaneously predicting stand-level *AGB*, *BGB*, and *ABGB*. In the case of MARS, two crucial hyperparameters, 'degree' and 'prune' require adjustment (Naser et al. 2022). The 'degree' represents the highest level of complexity, with 'degree' = 1 indicating a linear relationship and 'degree' $\geq$ 2 representing nonlinear interaction (Friedman 1991). However, an excessively high 'degree' can lead to overfitting, necessitating a careful balance between model complexity and available data. Regarding 'prune', it specifies the maximum quantity of terms in the pruned model, encompassing k hinge functions and the intercept. When 'degree' is set, and 'nprune' is NULL, the 'earth' function automatically selects predictive variables (X_{zh}), determines term numbers, and estimates values for the hinge function knots (c_{zh}), along with the parameters of coefficients (b_{ih}) and intercepts (a_i), streamlining the MARS model development process (Naser et al. 2022).

This approach employed cross-validation (details presented in the next section) for a range of MARS modeling systems using various 'degree' values ranging from 1 to 6. The outcomes of cross-validation supported selecting the optimal 'degree' value, ensuring that the MARS modeling system effectively captures both the goodness-of-fit and error metrics.

2.5. Deep Learning Additive Models (DLAMs)

The study introduced DLAMs, a formulation of DL models. These models can generate multiple outputs or predictions simultaneously, which is known as multi-output learning. The process involves training a deep neural network (DNN) to discern complex relationships and patterns within multi-inputs, facilitating predictions for multiple target variables. DLAMs map multiple inputs to various outputs, thus allowing for a more comprehensive analysis (Xu et al. 2020). Notably, DLAMs excel in capturing correlations and dependencies among output variables, leveraging shared information. By jointly training the DNN to make multiple predictions simultaneously, it extracts relevant features and relationships that contribute to all predictions. This simultaneous prediction of multiple outputs, informed by multi-input covariates, extends the model's applicability to complex decision-making problems. This approach resembles the method aiding in error reduction within the modeling system.

The operational mechanism of DLAMs as a multi-input multi-output learning system upgraded from single-output DL models (Huy et al. 2022b), and shares similarities with multi-output DL models (Huy et al. 2024). These models consist of multiple layers within DNNs, allowing the network to capture hierarchical representations of multi-input data (LeCun et al. 2015; Chollet 2018; Huy et al. 2022b). However, in a multi-output modeling framework, the final layer of the DNNs is explicitly configured to produce multiple outputs instead of a single output. Furthermore, in this study, DLAMs were tailored to consider correlations among errors of component models and ensure additivity when simultaneously predicting multiple outputs.

Various types of ANNs, including DNNs, convolutional neural networks (CNNs), and recurrent neural networks (RNNs), have been employed in DL models (LeCun et al. 2015; Huy et al. 2022b; Qin et al. 2023). Compared to traditional ANNs, DNNs feature a more intricate structure, comprising multiple layers of parameterized, distinct nonlinear modules trained using backpropagation (LeCun et al. 2015; Ogana and Ercanli 2021; Qin et al. 2023; Huy et al. 2024). Considering this, the study adopted the DNN architecture and developed multi-input multi-output deep neural networks (MODNNs) to create, cross-validate, and select the most suitable DLAMs.

The function system that expresses the MODNNs learning process for simultaneous multi-response predictions was adapted from Huy et al. (2022b, 2024). The modified function system is outlined as follows:

$$Y_{\text{multi-product j}} = \sum_{i=1}^{z} X_i \times w_i + \varepsilon_i \quad (8)$$

$$Y_{\text{multi-product}} = \left[Y_{\text{multi product 1}}, \ldots Y_{\text{multi-product j}}, \ldots, Y_{\text{multi-product ne}}\right] \quad (9)$$

$$Y_{\text{multi-output j}} = f\left(\sum_{i=1}^{z} X_i \times w_i + \varepsilon_i\right) \quad (10)$$

$$Y_{\text{multi-output}} = \left[Y_{\text{multi-output 1}}, \ldots Y_{\text{multi-output j}}, \ldots, Y_{\text{multi-output ne}}\right] \quad (11)$$

where $Y_{\text{multi-product j}}$ represents the multi-product at the j^{th} neuron among ne neurons of the neural network, $X_i = [X_1, X_2, \ldots X_i .., X_z]$ is the input vector with z predictive variables, w_i is the weight on the interconnection between X_i and the j^{th} neuron, ε_i represents the bias value, $Y_{\text{multi-product}}$ denotes the multi-product vector traversing through ne neurons of the neural network, $Y_{\text{multi-ouput j}}$ refers to the multi-output at the j^{th} neuron among the ne neurons of the neural network, f is the activation function applied at the j^{th} neuron, and $Y_{\text{multi-output}}$ represents the multi-output vector through ne neurons of the neural network.

The learning process of MODNNs facilitates the modeling of complex relational functions among multiple input variables, allowing for a comprehensive representation in the multi-output layer (LeCun et al. 2015; Huy et al. 2022b). This transformation is achieved through a parameterized layer with weights, as described by Huy et al. (2022b). The weights in the layer play a crucial role in capturing the relationships between the multi-inputs and generating accurate predictions for the multiple outputs within the MODNNs architecture. The learning process

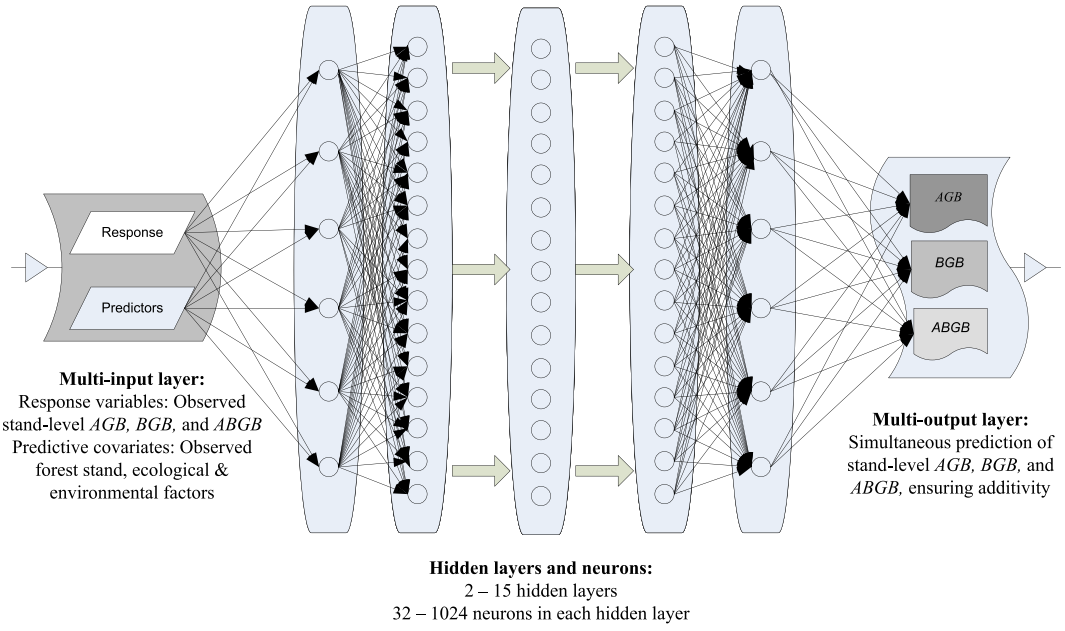

Fig. 4. Multi-Output Deep Neural Network (MODNN) simulation to simultaneously predict forest above- and belowground biomass and their total (*ABG*, *BGB* and *ABGB*, respectively), ensuring additivity, as Deep Learning Additive Models (DLAMs) with forest stand, ecological, and environmental factors as input predictive covariates.

Table 3
The primary analysis for selecting the algorithm, functions, hyperparameters and structure of the Multi-Output Deep Neural Network (MODNN).

ID	Elements	Minimum	Step	Maximum	Optimal selection
1	Batch	$32 = 2^5$	2^n with n = 5, 6	$64 = 2^6$	$32 = 2^5$
2	Epoch numbers	1000	1000	5000	3000
3	Learning rate	0.0001	0.001	0.01	0.001
4	Number of hidden layers	2	1	15	5
5	Number of neurons per hidden layer	$32 = 2^5$	2^n with n = 5, 6, 7, 8, 9 and 10	$1024 = 2^{10}$	$512 = 2^9$
6	Optimal algorithm	Adam, RMSprop, Stochastic Gradient Descent (SGD)			Adam optimizer
7	Patience	500	500	1500	1000
8	Scaling predictive variables	Non-scale, Normalization, Standardization			Non-scale

of MODNNs can be described as a multiple input and multiple output DL approach (Zhang et al. 2021). This characterization acknowledges the capability of the MODNNs to handle multiple input variables and generate multiple output predictions simultaneously, making it suitable for complex modeling tasks involving various inputs and outputs.

In this study, the MODNNs for the DLAMs were composed of multiple layers, including a multi-input layer with response variables of observed stand-level *AGB*, *BGB*, and *ABGB*, and predictive covariates of observed forest stand, ecological and environmental factors selected by FAMD. The hidden layers consisted of hundreds to thousands of neurons and a multi-output layer was responsible for simultaneously predicting stand-level *AGB*, *BGB* and *ABGB*. Fig. 4 depicts the simulated architecture of the MODNN for the DLAMs, an enhanced version built upon the DNN structure initially proposed by Huy et al. (2022b).

Choosing a suitable loss function (Huy et al., 2022b) to train and control the MODNNs for the DLAMs is crucial. In predicting forest biomass, emphasizing enhancing accuracy by reducing the percentage deviation, we selected the mean absolute percent error (Huy et al. 2022b) as our loss function ($MAPE_{loss}$, Eq. 12). This function aims to align the errors in predicting both stand-level *AGB* and *BGB* components simultaneously, along with an additional constraint loss that ensures the predicted total *ABGB* closely matches the combined sum of the observed stand-level *AGB* and *BGB* components (Huy et al. 2024).

$$\mathrm{MAPE}_{\mathrm{loss}}\ (\%) = \frac{100}{k}\sum_{j=1}^{k}\left\{\left|\frac{Y_{AGBj}-\widehat{Y}_{AGBj}}{Y_{AGBj}}\right| + \left|\frac{Y_{BGBj}-\widehat{Y}_{BGBj}}{Y_{BGBj}}\right| + \left|\frac{Y_{ABGBj}-\widehat{Y}_{ABGBj}}{Y_{ABGBj}}\right|\right\} \quad (12)$$

where; Y_{AGBj}, Y_{BGBj}, Y_{ABGBj} and $\widehat{Y}_{AGBj}$, $\widehat{Y}_{BGBj}$, and $\widehat{Y}_{ABGBj}$ were observed and predicted *AGB*, *BGB*, and *ABGB* for the j^{th} sample plot, respectively. k represented the total number of observed/predicted values from the validation or training dataset.

We used the One-Hot Encoding method to incorporate categorical variables into the MODNNs algorithms (Huy et al. 2022b). This encoding technique used the Pandas library's pd.get_dummies function (McKinney and Pandas Development Team 2022) to convert categorical variables into binary vectors. This transformation effectively utilizes categorical variables as inputs in the MODNNs modeling process, leveraging the functionality provided by Pandas' API.

The optimal MODNNs performance in this study was customized to suit the dataset's characteristics (Table 3), which are briefly described as follows: 1) *Scaling numeric covariates*: Three approaches were tested: i) Non-scaling; ii) Normalizing variables: The variables were divided by their maximum values and scaled to the range [0,1]; iii) Standardizing variables: The variables were standardized using the StandardScaler from the 'sklearn.preprocessing' module of the Python library (Huy et al. 2022b, 2024). The examination results indicated that for the given covariates, the non-scaling of numeric covariates was found to be more suitable and was chosen. 2) *Optimization algorithm*: Several key algorithms, including Adam, RMSprop, and Stochastic Gradient Descent (SGD) from the Keras library (Keras 2022), were evaluated to identify the best fit for achieving simultaneous predictions and actual multi-outputs. The results of the evaluation indicated that the Adam optimizer was chosen as the optimal algorithm for MODNNs. 3) *Learning rate selection*: The learning rate plays a crucial role in determining the extent

of weight adjustment during training (Huy et al. 2022b, 2024). In this study, the optimal learning rate of 0.001 was selected. 4) *Activation functions*: The selection of activation functions can greatly influence the performance of a MODNN (Bai 2022). Nonlinearity is vital in enabling MODNNs to effectively learn complex functional mappings from multi-inputs to multi-outputs. Among several popular activation functions such as Sigmoid, Tanh, Softmax, and Rectified Linear Unit (ReLU) (Sarker 2021), ReLU is commonly used in DNN architectures to introduce essential nonlinear properties (Bai 2022). This study chose the ReLU activation function from the Keras library (Keras 2022) for the hidden layers (Huy et al. 2022b, 2024). For the output layer, it is common practice to use a linear activation function (Huy et al. 2022b, 2024). 5) *The number of hidden layers*: The number of hidden layers in a MODNN can be adjusted to find the optimal depth for the specific task. The general structure of a DNN typically consists of two or more hidden layers (Sarker 2021). This study found that 5 layers yielded the best results. Additionally, a dropout layer with a parameter of 0.5 was applied to prevent overfitting and improve the generalization of the modeling system (Keras 2022). 6) *Number of neurons per hidden layer*: The number of neurons in each layer can be adjusted to control the model's complexity. This study determined that the optimal choice for each hidden layer was 512 neurons. 7) *Epoch numbers*: The number of epochs is a crucial hyperparameter that defines the number of times a deep learning algorithm iterates through the entire training dataset (Huy et al. 2022b, 2024). This study identified that the optimal choice was 3000 epochs. 8) *Batch size*: The batch size is an important hyperparameter that determines the number of training examples used in each training iteration (Huy et al. 2022b, 2024). In this study, the optimal choice was determined to be 32. 9) *An early stop function* with a patience parameter was implemented to halt the training when the validation loss ceased to decrease (Huy et al. 2022b), indicating the model's potential overfitting. After evaluation, a patience value of 1000 was determined to be the optimal choice.

The DLAMs codes were developed and implemented in Python (Python 2022), utilizing various Python libraries (Chollet 2018; Huy et al. 2022b, 2024). The code specifically utilized the Keras library (Keras 2022) in conjunction with Pandas (McKinney and Pandas Development Team 2022) for data manipulation and the TensorFlow backend (TensorFlow 2023) for deep learning operations (Chollet 2018; Huy et al. 2022b; Qin et al. 2023). We used these libraries' Application Programming Interfaces (APIs) and leveraged to define and train the MODNNs for simultaneous prediction of forest above- and belowground biomass. Python provided a flexible and powerful environment for implementing the MODNNs architecture and conducting the required DLAMs tasks.

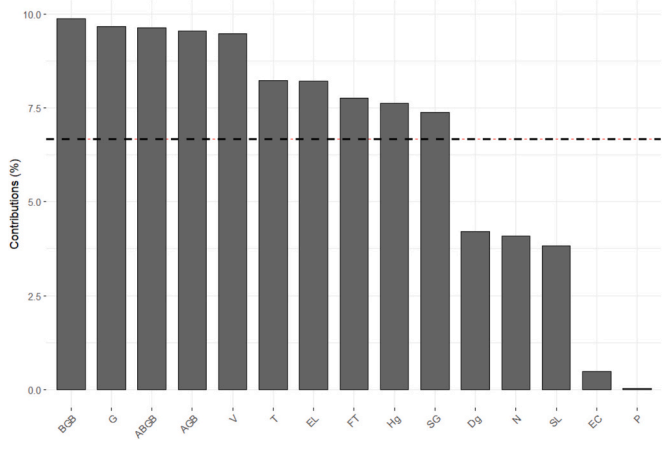

Fig. 5. FAMD results: Contribution percentage of 15 categorical nominal and numerical variables to the overall structure, with the average level indicated by a dashed line.
Note: *AGB*: aboveground biomass, *BGB*: belowground biomass, *ABGB*: above- and belowground biomass at stand-level. *G*: stand basal area per hectare. *V*: stand volume per hectare. *T*: mean annual temperature, *EL*: elevation, *FT*: forest type, DDF: Dry Dipterocarp Forest, EBLF: Evergreen Broadleaf Forest. *Hg*: average tree height corresponding to *Dg*. *SG*: soil group, FA: Ferric Acrisols, OA: Orthic Acrisols, RF: Rhodic Ferrasols. *Dg*: quadratic mean diameter at breast height. *N*: number of trees per hectare. *SL*: slope. *EC*: ecoregion, CH: Central Highlands, NCC: North Central Coast, NE: Northeast, SCC: South Central Coast, SE: Southeast. *P*: mean annual precipitation.

2.6. Selecting the optimal modeling systems

We developed various modeling systems in this study, including DLAMs, MARS, WNML, and WNSUR, utilizing different methods or approaches. The models were subjected to cross-validation to compare their performance and select the most optimal ones. The dataset was randomly divided into two subsets, allocating 70 % of the samples for training and reserving the remaining 30 % for validation. Cross-validation was performed ten times. We used the Akaike Information Criterion (AIC) (Akaike 1973), where lower AIC values indicate better fits to evaluate the adequacy of different equation forms. Additionally, the Fit Index (FI) was utilized as a goodness-of-fit measure, with values closer to 1 indicating superior model fits. To assess the reliability of the models, main error metrics were calculated, encompassing bias (%), root mean square error (RMSE, Mg ha^{-1}), and mean absolute percent error (MAPE, %), as described by Huy et al. (2022a, 2022b).

$$\text{Bias}\ (\%) = \frac{1}{C}\sum_{1}^{C}\frac{100}{k}\sum_{j=1}^{k}\frac{Y_j - \widehat{Y}_j}{Y_j} \tag{13}$$

$$\text{RMSE}\ \left(\text{Mg ha}^{-1}\right) = \frac{1}{C}\sum_{1}^{C}\sqrt{\frac{1}{k}\sum_{j=1}^{k}\left(Y_j - \widehat{Y}_j\right)^2} \tag{14}$$

$$\text{MAPE}\ (\%) = \frac{1}{C}\sum_{1}^{C}\frac{100}{k}\sum_{j=1}^{k}\left|\frac{Y_j - \widehat{Y}_j}{Y_j}\right| \tag{15}$$

$$\text{FI} = \frac{1}{C}\sum_{1}^{C}\left(1 - \frac{\sum_{j=1}^{k}\left(Y_j - \widehat{Y}_j\right)^2}{\sum_{j=1}^{k}\left(Y_j - \overline{Y}\right)^2}\right) \tag{16}$$

where C was the number of repeats (10) of cross-validation; k was the number of sample plots in the validation dataset (30 % randomly split dataset); and Y_j, $\widehat{Y}_j$ and $\overline{Y}$ were the observed, predicted, and averaged *AGB*, *BGB* and *ABGB* values, respectively, for the j^{th} sample plot of the validation dataset in realization C.

Bias and MAPE statistics, calculated using Eqs. (13) and (15), have been widely applied in forest biomass prediction evaluations (e.g., Huy et al. 2022b; Huy et al. 2023; Huy et al. 2024). In certain instances, these metrics tend to be biased towards negative errors (i.e., $Y_j < \widehat{Y}_j$) more than positive ones. To address this, metrics like the average systematic error (ASE) and mean percent standard error (MPSE) have been used, where the predicted rather than observed value is used in the denominator (Zeng et al. 2017, 2024; Huy et al. 2023). However, in the context of deep learning, we experimented with using predicted values in the denominator (Zeng et al. 2017, 2024) of the $\text{MAPE}_{\text{loss}}$. This approach tended to inflate the estimates to optimize the model, leading to substantial bias. Therefore, this study used Eqs. (13) and (15) with the observed values in the denominator. Additionally, an array of statistical metrics was applied to ensure the optimal selection of conventional regression forms.

The WNML, WNSUR, and MARS approaches employed cross-validation to compute averaged statistics and error metrics for their experimental modeling systems across 10 realizations. They then compared these metrics among the different models to identify the most

Table 4
Cross-validation for selecting independent component biomass models of stand-level *AGB*, *BGB*, and *ABGB* using different stand level predictors by weighted nonlinear maximum likelihood.

ID	Equation forms	Weight variable	AIC	FI	Bias (%)	RMSE (Mg ha^{-1})	MAPE (%)
AGB = f(Combinations of *G*, *V*, *Hg*)							
1	$AGB = a \times G^{b}$	$1/G^{\delta}$	808.9	0.950	−5.06	46.2	19.90
2	$AGB = a \times V^{b}$	$1/V^{\delta}$	719.1	0.969	−4.41	42.2	12.35
3	$AGB = a \times Hg^{b}$	$1/Hg^{\delta}$	951.5	0.580	−29.90	130.4	54.91
4	$AGB = a \times G^{b1} \times V^{b2}$	$1/G^{\delta}$	730.4	0.973	−1.89	35.7	10.77
5	$AGB = a \times G^{b1}Hg^{b2}$	$1/G^{\delta}$	761.7	0.948	−2.58	42.7	13.86
6	$\boldsymbol{AGB = a \times V^{b1}Hg^{b2}}$	$\boldsymbol{1/V^{\delta}}$	**713.5**	**0.979**	**−2.51**	**35.0**	**11.28**
7	$AGB = a \times G^{b1}V^{b2}Hg^{b3}$	$1/G^{\delta}$	747.5	0.974	−2.25	31.7	10.15
BGB = f(Combinations of *G*, *V*, *Hg*)							
1	$BGB = a \times G^{b}$	$1/G^{\delta}$	385.3	0.981	−9.37	2.2	16.23
2	$BGB = a \times V^{b}$	$1/V^{\delta}$	428.6	0.849	−6.12	7.9	14.45
3	$BGB = a \times Hg^{b}$	$1/Hg^{\delta}$	601.8	0.533	−15.29	10.8	37.25
4	$BGB = a \times (G \times V)^{b}$	$1/G^{\delta}$	387.5	0.950	−2.15	4.6	11.57
5	$\boldsymbol{BGB = a \times G^{b1}Hg^{b2}}$	$\boldsymbol{1/G^{\delta}}$	**375.5**	**0.977**	**−2.92**	**2.4**	**10.13**
6	$BGB = a \times V^{b1}Hg^{b2}$	$1/V^{\delta}$	419.5	0.725	−8.03	8.2	14.78
7	$BGB = a \times G^{b1}V^{b2}Hg^{b3}$	$1/G^{\delta}$	371.4	0.973	−5.33	2.3	12.25
ABGB = f(Combinations of *G*, *V*, *Hg*)							
1	$ABGB = a \times G^{b}$	$1/G^{\delta}$	815.0	0.951	−5.22	49.6	18.14
2	$ABGB = a \times V^{b}$	$1/V^{\delta}$	723.5	0.960	0.38	41.9	10.38
3	$ABGB = a \times Hg^{b}$	$1/Hg^{\delta}$	967.1	0.614	−35.40	146.7	55.68
4	$ABGB = a \times G^{b1} \times V^{b2}$	$1/G^{\delta}$	743.7	0.972	−1.15	33.8	9.15
5	$ABGB = a \times G^{b1}Hg^{b2}$	$1/G^{\delta}$	773.9	0.964	−1.79	41.2	11.81
6	$\boldsymbol{ABGB = a \times V^{b1}Hg^{b2}}$	$\boldsymbol{1/V^{\delta}}$	**725.3**	**0.968**	**−1.83**	**34.0**	**8.78**
7	$ABGB = a \times G^{b1}V^{b2}Hg^{b3}$	$1/G^{\delta}$	746.5	0.971	−1.31	37.6	9.58

Note: All statistics were calculated using cross-validation with 10 realizations, each repeating the dataset was split randomly into 70 % for training and 30 % for validation; statistics, and errors in mean results were averaged over ten times. *AGB* is aboveground biomass (Mg ha^{-1}), *BGB* is belowground biomass (Mg ha^{-1}), and *ABGB* is above- and belowground biomass (Mg ha^{-1}) at stand-level. *Hg* in m is the height of the tree with a *Dg* (the quadratic mean diameter at breast height), *G* is the stand basal area (m^2 ha^{-1}), and *V* is the volume of the stand (m^3 ha^{-1}). δ: the variance function coefficient. **Bold**: Selected model based on cross-validation statistics.

effective form.

In DL modeling, the DLAMs method opted for the finest model by minimizing the $MAPE_{loss}$ (Eq. 12). Employing the MODNNs framework, the model underwent training and validation phases. The MODNNs were exposed to 70 % of randomly segmented training data throughout the training and assessed against the remaining 30 %. This training regimen entailed iterating through the entire dataset 3000 times (epochs), with a batch size of 32. During each cross-validation iteration, training $MAPE_{loss}$ (Eq. 12) values were calculated for the training data at each epoch. The efficacy of the trained models was then assessed by computing validation $MAPE_{loss}$ (Eq. 12) values associated with the model's predictions at each epoch, which were subsequently compared with the actual values in each validation data. The best DLAMs was selected based on its performance across 10 cross-validation folds, prioritizing minimized $MAPE_{loss}$ on the validation data while ensuring consistency with training metrics. The statistics and error metrics of the selected model were computed to assess its effectiveness in the validation process, and the mean metrics were then calculated across the validation folds.

Furthermore, diagnostic plots were used to assess the performance of different modeling systems by comparing the trend of fitted/predicted values to observed values for stand-level *AGB*, *BGB*, and *ABGB*.

3. Results

3.1. Selected variables for modeling process

Following FAMD analysis, five variables, namely *Dg*, *N*, *SL*, *EC*, and *P* were found to contribute below the average level to the overall structure and demonstrated the lowest impact on the response variables stand-level *AGB*, *BGB*, and *ABGB* (Fig. 5). Consequently, these five predictive variables were excluded from the modeling process. Ten variables, exhibiting contributions above the average level to the overall variability, were included in the WNML, WNSUR, MARS, and DLAMs modeling process. These variables comprised three response variables, stand-level *AGB*, *BGB*, and *ABGB*, and seven predictive covariates: *G*, *V*, *T*, *EL*, *FT*, *Hg*, and *SG* (Fig. 5).

3.2. WNSUR associated with stand, ecological and environmental factors

The modeling systems were fitted using WNML and cross-validated to select the optimal equation forms for the independent biomass component models of stand-level *AGB*, *BGB*, and *ABGB*. Different stand predictor(s), or combinations of three stand covariates (*G*, *V*, and *Hg*) selected from FAMD were used. The results are represented in Table 4, which shows the comparison results based on cross-validation. To address the limitations of the bias and MAPE formulas in certain cases, we selected the final model forms based on multiple metrics, including AIC, FI, Bias, RMSE, and MAPE (Table 4). The best equation forms for predicting stand-level *AGB*, *BGB*, and *ABGB* separately were selected based on different combinations of stand covariates. Specifically, the combination of covariates (*V*, *Hg*) was chosen for the *AGB* model, (*G*, *Hg*) for the *BGB* model, and (*V*, *Hg*) for the *ABGB* model (Table 4).

The WNSUR equation system was formulated as $Biomass\ Component_i = Average_i \times Modifier_i$. In this equation, $Biomass\ Component_i$ represented the ith biomass component (stand-level *AGB*, *BGB*); $Average_i$ referred to the selected equation form of the ith biomass component, where $AGB = f(V, Hg)$ and $BGB = f(G, Hg)$ (Table 4); and $Modifier_i$ denoted the exponential function that adjusts the prediction of the biomass component i based on selected environmental and ecological factors from FAMD including four predictors: *T*, *EL*, *FT*, and *SG*. The WNSUR method was employed to develop the equation system that enables the simultaneous prediction of stand-level *AGB*, *BGB*, and *ABGB*, ensuring additivity. Cross-validation results for the WNSUR modeling systems are presented in Table 5. Based on FI, Bias, RMSE, and MAPE metrics, the selected best WNSUR system included six predictive covariates: *G*, *V*, *T*, *EL*, *Hg*, and *SG* (Table 5). This modeling system demonstrated statistically improved performance compared to the independent biomass component models

Table 5
Cross-validation of modeling systems of the *Biomass Component*$_i$ = *Average*$_i$ × *Modifier*$_i$ for simultaneously predicting stand-level *AGB*, *BGB* and *ABGB* associated with environmental and ecological variables fit by Weighted Nonlinear Seemingly Unrelated Regression (WNSUR).

ID	Simultaneous modeling system	Weight variable	FI	Bias (%)	RMSE (Mg ha^{-1})	MAPE (%)
1	$AGB = a_1V^{b11}Hg^{b12}\exp(e_{11}/100(T-22.9)+(e_{12}/1000)(EL-613)+e_{13}^{*}(FT-1.5)+e_{14}(SG-1.7))$	$1/V^{\delta}$	0.986	−2.48	29.2	9.06
	$BGB = a_2^{*}G^{b21}Hg^{b22*}\exp(e_{21}/100(T-22.9)+(e_{22}/1000)(EL-613)+e_{23}^{*}(FT-1.5)+e_{24}^{*}(SG-1.7))$	$1/G^{\delta}$	0.776	3.22	5.1	19.35
	$ABGB = AGB + BGB$	$1/G^{\delta}$	0.990	−1.63	29.5	8.74
2	$AGB = a_1V^{b11}Hg^{b12}\exp(e_{11}/100(T-22.9)+(e_{12}/1000)(EL-613)+e_{14}(SG-1.7))$	$1/V^{\delta}$	0.986	2.88	28.3	9.17
	$BGB = a_2G^{b21}\exp(e_{21}/100(T-22.9)+(e_{22}/1000)(EL-613))$	$1/G^{\delta}$	0.886	−3.30	4.2	18.31
	$ABGB = AGB + BGB$	$1/G^{\delta}$	0.989	1.99	29.1	7.71
3	$AGB = a_1V^{b11}Hg^{b12}\exp(e_{11}/100(T-22.9)+(e_{12}/1000)(EL-613)+e_{14}(SG-1.7))$	$1/V^{\delta}$	0.986	3.56	28.0	9.60
	$BGB = a_2G^{b21}$	$1/G^{\delta}$	0.886	−15.07	2.0	18.72
	$ABGB = AGB + BGB$	$1/G^{\delta}$	0.989	0.69	28.1	8.55

Note: The general form: *Biomass Component*$_i$ = *Average*$_i$ × *Modifier*$_i$ + ε_i; where *Average*$_i$ = the i^{th} independent model of *AGB/BGB* versus the stand variables of *G*, *V* and *Hg* selected by cross-validation; *Modifier*$_i$ is the i^{th} exponential function that helps adjust the prediction values of the biomass component *i* based on the environmental and ecological factors (T, EL, FT, SG) selected according to FAMD. *AGB* is the aboveground biomass (Mg ha^{-1}), *BGB* is the belowground biomass (Mg ha^{-1}), and *ABGB* is the above- and belowground biomass (Mg ha^{-1}) at stand-level. *G* is the stand basal area (m^2 ha^{-1}), *V* is the volume of the stand (m^3 ha^{-1}), and *Hg* in m is the height of the tree with a *Dg* (the quadratic mean diameter at breast height). *T* (°C year^{-1} averaged): mean annual temperature, *EL*: elevation (m), *FT*: forest type, DDF: Dry Dipterocarp Forest, EBLF: Evergreen Broadleaf Forest, *SG*: soil group, FA: Ferric Acrisols, OA: Orthic Acrisols, RF: Rhodic Ferrasols. All statistics were calculated using cross-validation, 70 % randomly split dataset for developing model system, and 30 % randomly split dataset for validating, finally, all metrics averaged over 10 realizations. δ: the variance function coefficient. **Bold**: The selected model system is based on cross-validation statistics and the significance of its parameter *p*-values.

* Parameter with *p* value > 0.05. The second modeling system excluded factors that had parameters with a *p*-value > 0.05.

Table 6
Estimated parameters of modeling systems: *Biomass Component*$_i$ = *Average*$_i$ × *Modifier*$_i$ for simultaneous estimations of stand-level *AGB*, *BGB* and *ABGB* using Weighted Nonlinear Seemingly Unrelated Regression (WNSUR) (based on the entire dataset).

ID	Modeling system	Parameters	Estimate ± Std. error	RMSE (Mg ha^{-1})	$R^2_{adj.}$
1	$AGB = a_1V^{b11}Hg^{b12}\exp(e_{11}/100(T-22.9)+(e_{12}/1000)(EL-613)+e_{13}(FT-1.5)+e_{14}(SG-1.7))$	a_1	2.005 ± 0.202	24.5	0.986
		b_{11}	1.003 ± 0.028		
		b_{12}	−0.3262 ± 0.0809		
		e_{11}	4.987 ± 0.671		
		e_{12}	0.4981 ± 0.0458		
		e_{13}^{*}	−0.09072 ± 0.05280		
		e_{14}	0.1216 ± 0.0180		
	$BGB = a_2G^{b21}Hg^{b22}\exp(e_{21}/100(T-22.9)+(e_{22}/1000)(EL-613)+e_{23}(FT-1.5)+e_{24}(SG-1.7))$	a_2^{*}	0.2375 ± 0.1625	8.4	0.771
		b_{21}	1.473 ± 0.172		
		b_{22}^{*}	−0.07703 ± 0.35150		
		e_{21}	−10.89 ± 3.26		
		e_{22}	−1.088 ± 0.237		
		e_{23}^{*}	0.05202 ± 0.28680		
		e_{24}^{*}	−0.1856 ± 0.1040		
	$ABGB = AGB + BGB$			23.3	0.989
2	$AGB = a_1V^{b11}Hg^{b12}\exp(e_{11}/100(T-22.9)+(e_{12}/1000)(EL-613)+e_{14}(SG-1.7))$	a_1	2.163 ± 0.191	24.5	0.986
		b_{11}	1.016 ± 0.027		
		b_{12}	−0.3900 ± 0.0758		
		e_{11}	4.785 + 0.634		
		e_{12}	0.4674 ± 0.0434		
		e_{14}	0.09325 ± 0.01340		
	$BGB = a_2G^{b21}\exp(e_{21}/100(T-22.9)+(e_{22}/1000)(EL-613))$	a_2	0.3312 ± 0.1061	6.0	0.885
		b_{21}	1.313 ± 0.086		
		e_{21}	−8.977 ± 2.405		
		e_{22}	−0.8707 ± 0.1867		
	$ABGB = AGB + BGB$			23.9	0.989

Note: The general form: *Biomass Component*$_i$ = *Average*$_i$ × *Modifier*$_i$ + ε_i; where *Average*$_i$ = the i^{th} independent model of *AGB/BGB* versus the stand variables of *G*, *V* and *Hg* selected by cross-validation; *Modifier*$_i$ is the i^{th} exponential function that helps adjust the prediction values of the biomass component *i* based on the environmental and ecological factors (*T*, *EL*, *FT*, *SG*) selected according to FAMD. *AGB* is the aboveground biomass (Mg ha^{-1}), *BGB* is the belowground biomass (Mg ha^{-1}), and *ABGB* is the above- and belowground biomass (Mg ha^{-1}) at stand-level. *G* is the stand basal area (m^2 ha^{-1}), *V* is the volume of the stand (m^3 ha^{-1}), and *Hg* in m is the height of the tree with a *Dg* (the quadratic mean diameter at breast height). *T* (°C year^{-1} averaged): Mean annual temperature, *EL*: Elevation (m), *FT*: Forest type, DDF: Dry Dipterocarp Forest, EBLF: Evergreen Broadleaf Forest, *SG*: Soil group, FA: Ferric Acrisols, OA: Orthic Acrisols, RF: Rhodic Ferrasols. **Bold**: The selected model system was based on cross-validation statistics and the significance of its parameter *p*-values.

* Parameter with *p* value > 0.05. The second modeling system excluded factors that had parameters with a *p*-value > 0.05.

for stand-level *AGB* and *ABGB*, with parameter significance indicated by a *p*-value of <0.05 (Table 5 vs. Table 4).

However, the WNSUR *BGB* component model, including the Modifier equation of the selected best WNSUR modeling system (Table 5), exhibited a poorer goodness-of-fit compared to the independent *BGB* model (Table 4). Therefore, the Modifier was removed from the WNSUR *BGB* model, and its cross-validation results are presented in Table 5. The results showed that the WNSUR *BGB* model with and without the Modifier had the same FI values, but the model with the Modifier outperformed the one without it in 5 of the 9 component-metrics combinations. Thus, removing the Modifier from the *BGB* model in the WNSUR modeling system did not improve the goodness-of-fit of the WNSUR *BGB* model compared to the independent *BGB* model without the Modifier (Table 5 vs. Table 4). This can be explained by the nature of the WNSUR approach, which considers the biological relationship between *AGB*, *BGB*, and total *ABGB* to harmonize the reliability of the estimates for each component, focusing on minimizing the error for the total *ABGB* function and ensuring additivity. In this study, the selected best WNSUR modeling system with Modifiers led to significant improvements in the *AGB* and *ABGB* models, while the *BGB* model exhibited a poorer goodness-of-fit compared to the independent component models without Modifiers (Table 5 vs. Table 4).

The estimated parameters of the modeling systems for the simultaneous prediction of stand-level *AGB*, *BGB*, and *ABGB*; with models fitted by WNSUR using the entire dataset, are shown in Table 6. In practical applications, variable *V* needs to be converted from stand-level measurements to aboveground and belowground biomass. Consequently, a WNSUR modeling system utilizing the entire dataset was developed to simultaneously predict stand-level *AGB*, *BGB*, and *ABGB* using the single

Table 7
Estimated parameters of a modeling system for simultaneous estimation of stand-level *AGB*, *BGB* and *ABGB* versus only stand predictive variable of *V* using Weighted Nonlinear Seemingly Unrelated Regression (WNSUR), including cross-validation results.

Modeling system	Parameters	Estimate ± Std. error	FI	Bias (%)	RMSE (Mg ha^{-1})	MAPE (%)
$AGB = a_1 V^{b11}$	a_1	0.6450 ± 0.0893	0.966	10.78	35.9	15.26
	b_{11}	1.053 ± 0.0210				
$BGB = a_2 V^{b21}$	a_2	0.8207 ± 0.0729	0.924	−16.05	4.2	21.86
	b_{21}	0.6457 ± 0.0138				
$ABGB = AGB + BGB$			0.967	6.91	38.0	11.21

Note: *AGB* is the aboveground biomass (Mg ha^{-1}), *BGB* is the belowground biomass (Mg ha^{-1}), and *ABGB* is the above- and belowground biomass (Mg ha^{-1}) at stand-level. *V* is the stand volume (m^3 ha^{-1}). Weight variable = 1 / V$^{\delta}$. All parameters have a *p*-value < 0.0001. The modeling system parameters were estimated using the entire dataset. All statistical metrics were calculated using cross-validation, 70 % randomly split dataset for developing model system, and 30 % randomly split dataset for validating, finally, all metrics averaged over 10 realizations.
$^{\delta}$ The variance function coefficient.

Table 8
Cross-validation metrics of Multivariate Adaptive Regression Splines (MARS) modeling systems with different 'degree' values and 'nprune' set to NULL for determining the optimal 'degree' in the modeling system associated with the number of optimal terms and predictors.

Degree	FI	Bias (%)	RMSE (Mg ha^{-1})	MAPE (%)	Selected nprune (terms)	Selected predictors
1	0.975	−0.85	35.3	10.30	7/9	4/7
2	**0.982**	**−0.36**	**29.6**	**9.41**	**9/11**	**5/7**
3	0.976	−1.35	36.7	10.40	9/11	5/7
4	0.979	−1.56	34.8	10.49	9/11	5/7
5	0.980	1.08	36.9	10.56	9/11	5/7
6	0.975	−1.15	40.8	10.59	9/11	5/7

Note: The cross-validation statistics are for predicting stand-level above- and belowground biomass (ABGB, Mg ha^{-1}); each repeating dataset was split randomly into 70 % for training and 30 % for validation; finally, all statistics, and error metrics averaged over 10 realizations. **Bold**: The optimal 'degree' value in the best MARS modeling.

variable *V*, and the corresponding results are presented in Table 7. However, it should be noted that the modeling system utilizing only variable *V* exhibited higher error metrics compared to the best modeling system incorporating the complete set of optimized variables, which included forest stand, environmental, and ecological factors such as *G*, *V*, *Hg*, *T*, *EL*, and *SG* (Table 7 vs. Table 5).

3.3. MARS associated with stand, ecological, and environmental factors

Using cross-validation and exploring a range of 'degree' hyper-parameter values based on FI, Bias, RMSE, and MAPE, the optimal MARS equation system, which exhibited superior performance across these four statistical measures, was determined with a 'degree' hyper-parameter set to 2 (Table 8). The best modeling system incorporates nine terms and uses five optimal predictors: *V*, *Hg*, *G*, *T*, and *EL*. These findings, presented in Table 8, Table 9 and Fig. 6, indicate that the optimal model is nonlinear, suggesting a complex relationship between the predictors and responses. Table 9 represents the determination of the hinge functions and their estimated coefficients of the optimal MARS equation system, accompanied by the cross-validation metrics for each predicted response. The FI values for MARS were 0.981, 0.956, and 0.982 for simultaneously predicting stand-level *AGB*, *BGB*, and *ABGB*, respectively (Table 9).

3.4. DLAMs associated with stand, ecological and environmental factors

Various combinations of predictive covariates selected by FAMD, including *G*, *V*, *T*, *EL*, *FT*, *Hg*, and *SG*, were utilized. Ten DLAMs were created using these seven covariates (Table 10). Initially, DLAMs 1 was developed with all seven predictive covariates. Subsequently, the covariate(s) with the lowest contribution (Fig. 5) was gradually eliminated

Table 9
The estimated intercepts, coefficients and knot values for hinge functions of the Multivariate Adaptive Regression Splines (MARS) best modeling system, based on the entire dataset using five selected predictors (*V*, *Hg*, *G*, *T*, and *EL*) with degree = 2, nprune = 9, for simultaneous prediction of stand-level *AGB*, *BGB*, and *ABGB*, along with cross-validation statistics.

Terms (basis/hinge functions)	*AGB*	*BGB*	*ABGB*
	Coefficients		
Intercept	402.9	12.96	415.86
$h(17.1 - G)$	−1.455	−1.163	−2.619
$h(G - 17.1)$	3.200	0.9495	4.150
$h(554.1 - V)$	−0.6917	0.007186	−0.6846
$h(V - 554.1)$	0.9304	−0.009269	0.9211
$h(EL - 390)$	0.04140	0.004565	0.04600
$h(Hg - 15.7)$	−20.20	−0.02322	−20.23
$h(G - 17.1) \times h(T - 21.7)$	−1.0950	0.02627	−1.069
$h(G - 17.1) \times h(21.7 - T)$	−0.2731	−0.01529	−0.2884
Fit index (FI) and error metrics			
FI	0.981	0.956	0.982
Bias (%)	0.73	−7.11	−0.36
RMSE (Mg ha^{-1})	28.1	3.6	29.6
MAPE (%)	10.61	15.91	9.41

Note: $h(X_{zh} - c_{zh})$ or $h(c_{zh} - X_{zh})$ refers to the hinge function is an essential component of the MARS modeling system and represents a specific mathematical form, where X_{zh} is the z^{th} selected predictor such as *G*, *V*, *EL*, *Hg* and *T* in the h^{th} function, and 'c_{zh}' is a knot value associated with the z^{th} predictor for the hth function.
AGB (Mg ha^{-1}): aboveground biomass, *BGB* (Mg ha^{-1}): belowground biomass, *ABGB* (Mg ha^{-1}): above- and belowground biomass at stand-level, *Hg* (m): the height of the tree with a *Dg* (the quadratic mean diameter at breast height), *G* (m^2 ha^{-1}): stand basal area per hectare, *V* (m^3 ha^{-1}): stand volume per hectare, *EL*: elevation (m), *T* (°C year^{-1} averaged): mean annual temperature. All statistics and error metrics were calculated using the cross-validation, 70 % randomly split dataset for training models, and 30 % randomly split dataset for validating, and averaged over 10 realizations.

until only one key stand variable, with the highest impact on responses of stand-level *AGB*, *BGB*, and *ABGB*, either *G* or *V* (Fig. 5), remained, resulting in the modeling systems named DLAMs 9 and DLAMs 10, respectively (Table 10).

Table 10 show the cross-validation metrics for the developed and validated DLAMs (DLAMs 1–10). All ten DLAMs achieved high FIs above 0.95, indicating good fits (Table 10). After evaluating the goodness-of-fit and error metrics – FI, Bias, RMSE and MAPE – and analyzing the plots of fitted versus observed stand-level *AGB*, *BGB*, and *ABGB* for the ten DLAMs (Fig. 7), it was determined that the best modeling system was DLAMs 1, which incorporated seven predictive covariates including *G*, *V*, *T*, *EL*, *FT*, *Hg*, and *SG*. This DLAMs 1 modeling system achieved a good fit with FI of 0.986, 0.989, and 0.987, along with low MAPEs of 6.29 %, 4.27 %, and 5.28 % for the simultaneous prediction of stand-level *AGB*, *BGB*, and *ABGB*, respectively (Table 10).

In practice, stand volume *V* is commonly the primary attribute found

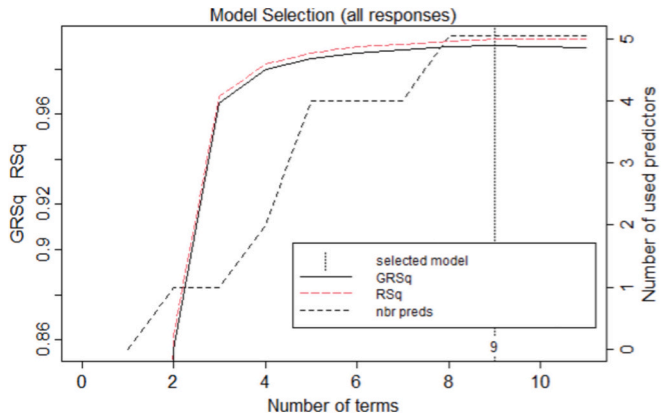

Fig. 6. Depicts the Generalized R-Squared (GRSq) and R-Squared (RSq) of the Multivariate Adaptive Regression Splines (MARS) modeling system as a function of the number of terms and used predictors. The plot highlights the selected model with a degree of 2 that attained the highest GRSq/RSq value, achieved with 9 terms (nprunes) and utilizing 5 predictors.

in forest resource databases. This attribute varies based on forest statuses and can be influenced by various disturbance levels. Therefore, DLAMs 10, which incorporated only the *V* covariate, was utilized to simultaneously predict stand-level *AGB*, *BGB*, and *ABGB* to observed *V* classes. Table 11 provides the predictions for the two biomass carbon pools, aboveground and belowground, and their total in Vietnam's tropical forest statuses, with the biomass, carbon sequestration, and equivalent CO_2 (CO_2e) absorption showing variations ranging from 13 to 994 Mg ha^{-1}, from 6 to 467 Mg ha^{-1}, and from 22 to 1714 Mg ha^{-1}, respectively.

4. Discussion

4.1. DLAMs vs. WNSUR, MARS and ML modeling systems

Genc et al. (2023) highlighted that the use of ANN approaches for estimating tree biomass surpassed the performance of regression methodology. However, our study delved deeper by developing DLAMs using MODNNs. These MODNNs exhibited enhanced robustness and innovation compared to traditional ANNs. Our research also conducted a comparative analysis, evaluating DLAMs against statistical approaches such as the WNSUR and MARS methods. All three approaches – DLAMs, WNSUR, and MARS – utilized multiple predictors encompassing forest stand variables, ecological and environmental factors. They simultaneously predicted stand-level *AGB*, *BGB*, and *ABGB*, ensuring additivity, within tropical mixed-species forests.

Table 12 compares the three optimal modeling systems – DLAMs, MARS, and WNSUR based on cross-validation results. Four statistical and error metrics – FI, Bias, RMSE, and MAPE were used for the comparison. The results showed that the DLAMs system outperforms the other two modeling systems, with most of the four metrics being superior. Meanwhile, the MARS and WNSUR systems exhibited very similar results across these metrics, indicating that neither approach was superior in terms of goodness-of-fit or error metrics.

In forest biomass carbon prediction, minimizing percentage deviation is crucial, as indicated by MAPE values. Consequently, when comparing the modeling systems, this error metric was prioritized, favoring the selection of models with lower MAPE values across the components (Huy et al. 2022b). Using the best DLAMs 1, which employed seven optimal covariates (*G*, *V*, *T*, *EL*, *FT*, *Hg*, and *SG*), the MAPEs for simultaneously predicting stand-level *AGB*, *BGB*, and *ABGB* decreased by 2.9 %, 14.0 %, and 2.4 %, respectively, compared to the best WNSUR modeling system, which incorporated six optimal predictive variables (*G*, *V*, *T*, *EL*, *Hg*, and *SG*) (Table 12). Specifically, the

Table 10
The optimal Deep Learning Additive Models (DLAMs) of different combinations of predictive covariates for simultaneously predicting stand-level *AGB*, *BGB*, and *ABGB* — cross-validation statistics.

ID	DLAMs code	Combinations of predictive covariates	FI	Bias (%)	RMSE (Mg ha^{-1})	MAPE (%)
1.	**DLAMs 1**	**7 predictive covariates: *G, V, T, EL, FT, Hg, SG***				
		Optimal metrics				
		Predicting *AGB*	0.986	−1.57	22.8	6.29
		Predicting *BGB*	0.989	−0.81	1.6	4.27
		Predicting *ABGB* = *AGB* + *BGB*	0.987	−1.38	16.2	5.28
		Mean metrics				
		Predicting *AGB*	0.982	−1.17	26.3	7.55
		Predicting *BGB*	0.981	0.15	2.3	4.94
		Predicting *ABGB* = *AGB* + *BGB*	0.983	−0.86	18.7	6.57
2.	DLAMs 2	6 predictive covariates: *G, V, T, EL, FT, Hg*				
		Optimal metrics				
		Predicting *AGB*	0.976	−2.61	22.4	6.94
		Predicting *BGB*	0.989	1.84	1.5	3.53
		Predicting *ABGB* = *AGB* + *BGB*	0.980	−1.88	15.9	5.89
		Mean metrics				
		Predicting *AGB*	0.978	−0.81	30.5	7.53
		Predicting *BGB*	0.968	−0.44	2.9	6.24
		Predicting *ABGB* = *AGB* + *BGB*	0.980	−0.58	21.7	6.63
3.	DLAMs 3	6 predictive covariates: *G, V, T, EL, Hg, SG*				
		Optimal metrics				
		Predicting *AGB*	0.992	1.00	18.2	5.96
		Predicting *BGB*	0.989	−0.13	2.0	4.48
		Predicting *ABGB* = *AGB* + *BGB*	0.993	1.00	13.0	5.29
		Mean metrics				
		Predicting *AGB*	0.985	−1.27	23.9	7.43
		Predicting *BGB*	0.978	−0.94	2.1	4.76
		Predicting *ABGB* = *AGB* + *BGB*	0.986	−1.07	17.0	6.51
4.	DLAMs 4	5 predictive covariates: *G, V, T, EL, FT*				
		Optimal metrics				
		Predicting *AGB*	0.987	1.17	25.3	4.61
		Predicting *BGB*	0.945	−0.42	4.3	6.16
		Predicting *ABGB* = *AGB* + *BGB*	0.987	1.10	18.1	4.32
		Mean metrics				
		Predicting *AGB*	0.975	1.27	29.1	8.16
		Predicting *BGB*	0.971	1.88	2.8	6.10
		Predicting *ABGB* = *AGB* + *BGB*	0.978	1.51	20.7	7.23
5.	DLAMs 5	5 predictive covariates: *G, V, T, EL, Hg*				
		Optimal metrics				
		Predicting *AGB*	0.986	−1.27	19.4	6.07
		Predicting *BGB*	0.984	0.72	2.0	4.99
		Predicting *ABGB* = *AGB* + *BGB*	0.988	−0.84	13.8	5.12
		Mean metrics				
		Predicting *AGB*	0.979	−0.44	26.3	7.37
		Predicting *BGB*	0.980	0.75	2.3	5.45
		Predicting *ABGB* = *AGB* + *BGB*	0.981	−0.13	18.6	6.49
6.	DLAMs 6	4 predictive covariates: *G, V, T, EL*				
		Optimal metrics				
		Predicting *AGB*	0.986	−0.68	24.7	6.07
		Predicting *BGB*	0.995	−0.90	1.1	3.10
		Predicting *ABGB* = *AGB* + *BGB*	0.988	−0.66	17.5	5.22
		Mean metrics				
		Predicting *AGB*	0.971	0.44	31.8	7.57
		Predicting *BGB*	0.941	0.54	3.7	5.67
		Predicting *ABGB* = *AGB* + *BGB*	0.971	0.58	22.7	6.75
7.	DLAMs 7	3 predictive covariates: *G, V, T*				
		Optimal metrics				
		Predicting *AGB*	0.985	−0.43	19.0	6.98
		Predicting *BGB*	0.994	1.01	1.1	2.86

(*continued on next page*)

Table 10 (*continued*)

ID	DLAMs code	Combinations of predictive covariates	FI	Bias (%)	RMSE (Mg ha^{-1})	MAPE (%)
		Predicting *ABGB* = *AGB* + *BGB*	0.988	−0.11	13.5	6.04
		Mean metrics				
		Predicting *AGB*	0.981	0.27	27.5	7.90
		Predicting *BGB*	0.986	0.59	2.0	4.37
		Predicting *ABGB* = *AGB* + *BGB*	0.984	0.46	19.5	6.91
8.	DLAMs 8	2 predictive covariates: *G*, *V*				
		Optimal metrics				
		Predicting *AGB*	0.963	−0.15	44.7	7.24
		Predicting *BGB*	0.997	0.31	1.0	3.44
		Predicting *ABGB* = *AGB* + *BGB*	0.968	0.08	31.6	6.05
		Mean metrics				
		Predicting *AGB*	0.949	0.14	47.0	9.23
		Predicting *BGB*	0.988	0.38	1.8	4.11
		Predicting *ABGB* = *AGB* + *BGB*	0.957	0.37	33.3	8.01
9.	DLAMs 9	1 predictive variable: *G*				
		Optimal metrics				
		Predicting *AGB*	0.977	1.52	33.4	13.52
		Predicting *BGB*	0.983	−0.68	2.3	9.34
		Predicting *ABGB* = *AGB* + *BGB*	0.980	1.50	23.7	12.65
		Mean metrics				
		Predicting *AGB*	0.931	3.72	57.1	17.69
		Predicting *BGB*	0.981	2.16	2.4	10.92
		Predicting *ABGB* = *AGB* + *BGB*	0.942	3.88	40.4	16.42
10.	DLAMs 10	1 predictive variable: *V*				
		Optimal metrics				
		Predicting *AGB*	0.973	3.43	33.8	8.59
		Predicting *BGB*	0.947	1.60	4.1	9.23
		Predicting *ABGB* = *AGB* + *BGB*	0.973	3.33	24.1	8.12
		Mean metrics				
		Predicting *AGB*	0.960	−2.22	41.8	10.48
		Predicting *BGB*	0.864	−1.50	6.2	10.39
		Predicting *ABGB* = *AGB* + *BGB*	0.959	−1.95	29.9	9.91

Note: *AGB*: aboveground biomass (Mg ha^{-1}), *BGB*: belowground biomass (Mg ha^{-1}), and *ABGB* above- and belowground biomass (Mg ha^{-1}) at stand-level. *G*: Stand basal area per hectare (m^2 ha^{-1}), *V*: stand volume per hectare (m^3 ha^{-1}), *T*: mean annual temperature (°C year^{-1} averaged), *EL*: elevation (m), *FT*: forest type, DDF: Dry Dipterocarp Forest, EBLF: Evergreen Broadleaf Forest, *Hg* (m): height of the tree with a *Dg* (the quadratic mean diameter at breast height), *SG*: soil group, FA: Ferric Acrisols, OA: Orthic Acrisols, RF: Rhodic Ferrasols.
Selection of modeling systems through cross-validation involved 10 repetitions, with the dataset split randomly into 70 % for training and 30 % for validation each time; the optimal DLAMs was selected based on its performance across 10 cross-validation folds, and its statistics and error metrics were computed to assess its effectiveness in the validation process; and the mean metrics were then calculated across the validation folds. **Bold:** The best-selected DLAMs modeling system.

MAPEs from the DLAMs 1 reduced by 4.3 %, 11.6 %, and 4.1 % compared to the best MARS system, which included five optimal predictive variables (*G*, *V*, *T*, *EL*, and *Hg*) for simultaneously predicting stand-level *AGB*, *BGB*, and *ABGB*, respectively (Table 12). Fig. 8 demonstrates a clear improvement in the fits of the DLAMs approach compared to the WNSUR and MARS methods. The DLAMs exhibit noticeably better fits, indicating its better performance in capturing the relationship between predictors and forest biomass components.

When comparing the *V*-based modeling systems, DLAMs 10 (Table 10) outperformed WNSUR (Table 7) across 7 out of 12 component-metrics combinations from cross-validation. Additionally, DLAMs 10 exhibited improved MAPE values across all three component models compared to the WNSUR *V*-based system, highlighting that reductions in MAPE are essential for accurate forest biomass predictions. Consequently, the DLAMs system demonstrated a superior goodness-of-fit relative to the WNSUR modeling system when using a sole *V* predictor. However, the WNSUR *V*-based system is simpler to apply and has slightly lower reliability than DLAMs 10. Therefore, WNSUR models are recommended for parsimony when using only the *V* predictor.

The results presented here differ from the findings of Qin et al. (2023), who suggested that DL modeling has lower reliability than regression modeling when using the same predictive variables. According to their study, DL modeling exhibits high reliability only when incorporating many predictive covariates. On the contrary, we believe this discrepancy may be related to the design of the DNN or MODNNs, including selecting appropriate structures, algorithms, and hyperparameters tailored to the research data.

The comparison results between the DLAMs approach and regression modeling, such as WNSUR, in this study align with several publications by Ercanli (2020) and Huy et al. (2022b, 2024), indicating that DL modeling demonstrates significant advantages over the regression approach. One notable advantage of the DL approach is that it does not require finding an optimal function like traditional regression methods. This is particularly advantageous because the relationships between tropical rainforest biomass and ecological environmental factors are complex and poorly understood. Through DNN, DL modeling can detect patterns in these relationships and make predictions with minor errors. Additionally, DL modeling does not rely on normally distributed variables and does not require handling heteroscedasticity issues in predicted variables. It can also handle nominal categorical variables by encoding them into binary vectors (Huy et al. 2022b, 2024; Qin et al. 2023).

The MARS modeling system shares the same advantages as DLAMs, being a non-parametric regression approach, which offers distinct advantages compared to parameter regression methods like WNSUR. MARS does not require the assumption of variable normality and can identify suitable functional forms (Laurin et al. 2016). Like DLAMs, it can also handle numeric and nominal categorical variables, exhibiting a flexible and versatile form (Yasmirullah et al. 2021). MARS is particularly effective when dealing with many responses and predictor variables in the modeling process (Koc and Bozdogan 2015). This study also examined the additivity of simultaneously predicted responses from the MARS equation systems, resulting in the relationship *ABGB* = *AGB* + *BGB* being verified. Therefore, MARS has found applications in various multivariate regression models and has been reported to outperform other modeling algorithms in certain scenarios (Arjasakusuma et al. 2020). The MARS method excels automatically selecting the number of significant predictive variables — a function that surpasses DLAMs. Moreover, it develops nonlinear relationships by selecting hinge functions, which are a key component in the MARS model.

In contrast, this poses a challenge for parametric regression like WNSUR, where determining the appropriate number of predictors and capturing nonlinear relationships requires more manual intervention. By looking at cross-validation data, we saw that most error measurements for MARS were the same as those for WNSUR (Table 12). This suggests that MARS and WNSUR generally predict with similar accuracy. However, MARS has its strengths, showing potential in creating models that predict multiple connected results simultaneously. The MARS approach utilizes complex input data with relationships that are hard to find.

Furthermore, a recent study utilized ML techniques to predict the total stand biomass, including both aboveground and belowground components, in natural coniferous-broadleaved mixed forests in China. The study incorporated multiple variables, such as stand characteristics, climate, and soil factors, as predictors, achieving promising results with an R^2 value of 0.89 (He et al. 2023). In our study, the use of DLAMs demonstrated significantly better performance than ML, with an FI (R^2) exceeding 0.98. Additionally, DLAMs enable simultaneous predictions of aboveground, belowground, and total stand-level biomass in contrast

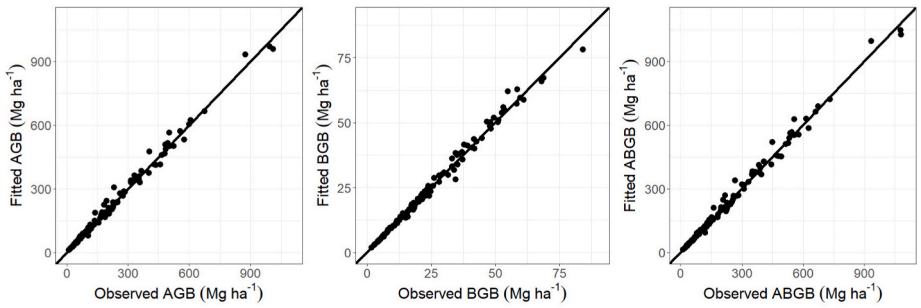

DLAMs 1: 7 predictive covariates: *G, V, T, EL, FT, Hg, SG*

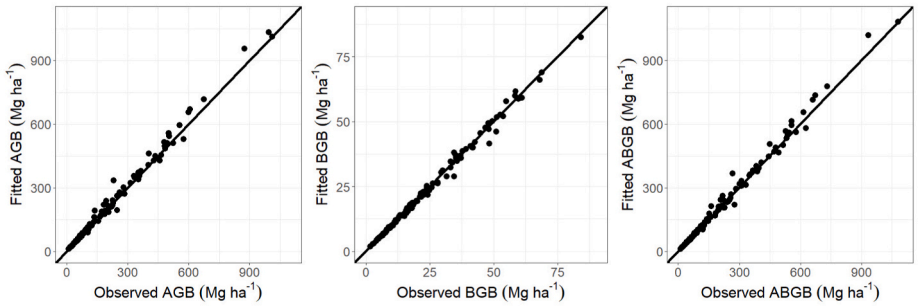

DLAMs 2: 6 predictive covariates*: G, V, T, EL, FT, Hg*

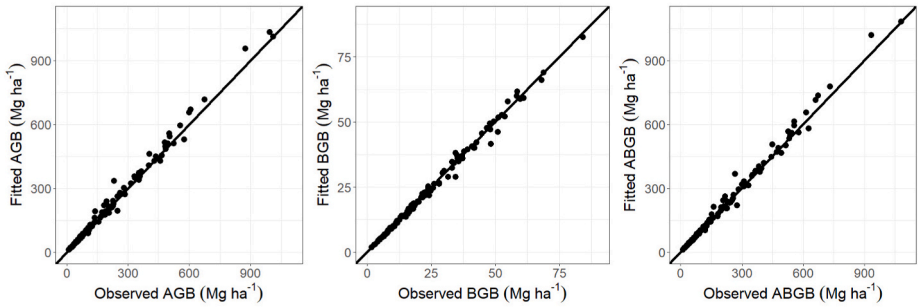

DLAMs 3: 6 predictive covariates: *G, V, T, EL, Hg, SG*

Fig. 7. Plots of fitted vs. observed values of DLAMs for simultaneous estimations of stand-level *AGB*, *BGB*, and *ABGB* using different combinations of predictors selected by FAMD analysis, based on the entire dataset.
Note: *AGB*: aboveground biomass (Mg ha^{-1}), *BGB*: belowground biomass (Mg ha^{-1}), and *ABGB*: above- and belowground biomass (Mg ha^{-1}) at stand-level. *G*: stand basal area per hectare (m^2 ha^{-1}), *V*: stand volume per hectare (m^3 ha^{-1}), *T*: mean annual temperature (°C year^{-1} averaged), *EL*: elevation (m), *FT*: forest type, DDF: Dry Dipterocarp Forest, EBLF: Evergreen Broadleaf Forest, *Hg* (m): height of the tree with a *Dg* (the quadratic mean diameter at breast height), *SG*: soil group, FA: Ferric Acrisols, OA: Orthic Acrisols, RF: Rhodic Ferrasols.

to ML techniques, with typically predict these components or totals separately.

In recent years, the application of DL models has successfully addressed various challenges across multiple fields, as mentioned by Sarker (2021). Nevertheless, the development and application of DL models in terms of biometrics, forest carbon biomass dynamics, and forest ecology modeling are still in their early stages. Given the numerous advantages of DL modeling in general, as demonstrated in this study, it is crucial to recognize DL as a significant alternative approach for capturing complex relationships within tropical forest biomass carbon and ecology. Both parametric and non-parametric regressions have their advantages, but DL has unique capabilities that make it particularly well-suited for handling the complexities associated with these relationships. DL's ability to automatically learn intricate patterns and representations from data and its capacity to model highly nonlinear relationships makes it a powerful tool for various predictive modeling tasks.

In the realm of DL methodology for regression, it's important to acknowledge that while MODNNs techniques facilitate the development of DLAMs that outperform equation systems produced by conventional regression methods, they do have certain limitations. For instance, they cannot automatically select significant predictive covariates for modeling DLAMs, and the thorough examination and selection of the appropriate MODNNs architecture that determines the reliability and error of the DLAMs can be time-consuming.

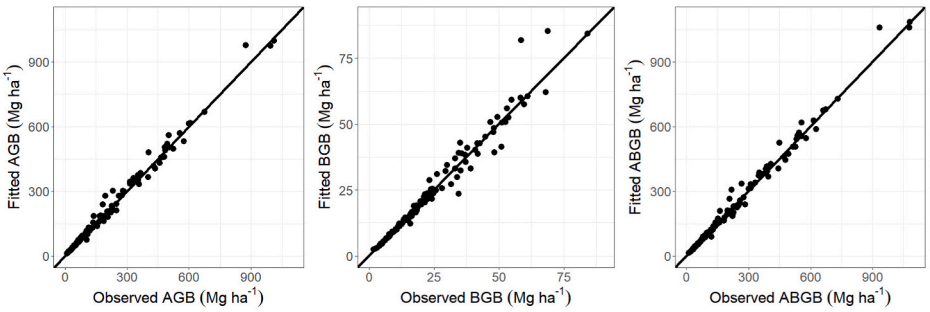

DLAMs 4: 5 predictive covariates: *G, V, T, EL, FT*

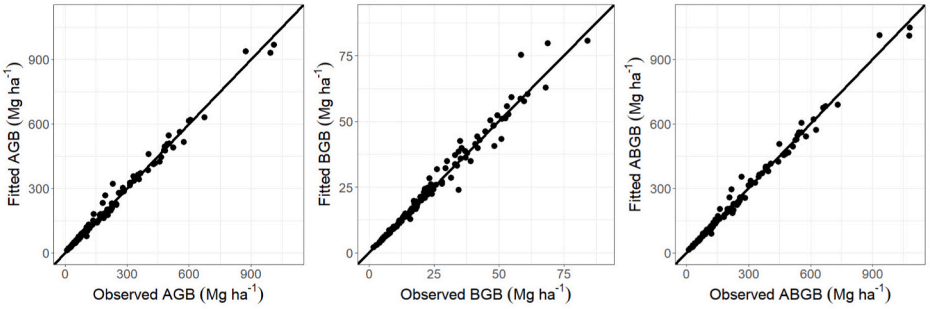

DLAMs 5: 5 predictive covariates: *G, V, T, EL, Hg*

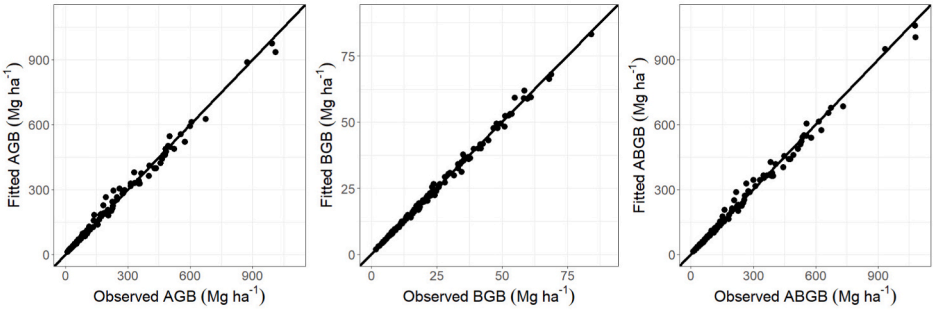

DLAMs 6: 4 predictive covariates: *G, V, T, EL*

Fig. 7. (*continued*).

4.2. Designing MODNNs to achieve greater reliability of DLAMs

In the context of utilizing DLAMs to predict stand-level *AGB*, *BGB*, and *ABGB* simultaneously, thoroughly examining and selecting appropriate MODNNs that align with the specific research data is crucial. Different MODNNs designs result in notable variations in the reliability and error of the DLAMs.

Designing MODNNs includes experimenting with the dataset across key components such as 1) Selecting a scaling method for predictive covariates to ensure they have an equal impact on the response variables; 2) The selection of an optimization algorithm is crucial (Qin et al. 2023; Huy et al. 2024;) as it plays a significant role in ensuring that DLAMs is capable of identifying the best-fitting modeling system. Alongside this, choosing an appropriate learning rate that suits the input data is also important; 3) The selection of activation functions plays a crucial role, especially when dealing with nonlinear relationships between forest biomass and predictor variables in ecological environments. Therefore, in many cases, the Rectified Linear Unit (ReLU) activation function (Huy et al. 2022b, 2024; Qin et al. 2023) is suitable for hidden layers, as it can capture complex patterns effectively. Simultaneously, a linear activation function is appropriate for the output layer, ensuring a close linear relationship between observed and predicted output values; 4) Designing the structure of MODNNs with the adjustment of the number of hidden layers and neurons per hidden layer is crucial (Ercanli 2020; Ogana and Ercanli 2021; Huy et al. 2022b, 2024; Qin et al. 2023) for different datasets. Conducting investigations to select the appropriate number of hidden layers and neurons significantly influences the reliability of predictions for the output variables; 5) Hyperparameters such as epoch, batch size, and patience need to be adjusted (Huy et al. 2022b, 2024; Qin et al. 2023; Seely et al. 2023) according to the observed data and the level of relationship between the response variables and covariates. These hyperparameters determine how the data is utilized, the number of iterations the computer learns, and when to stop appropriately to avoid overfitting.

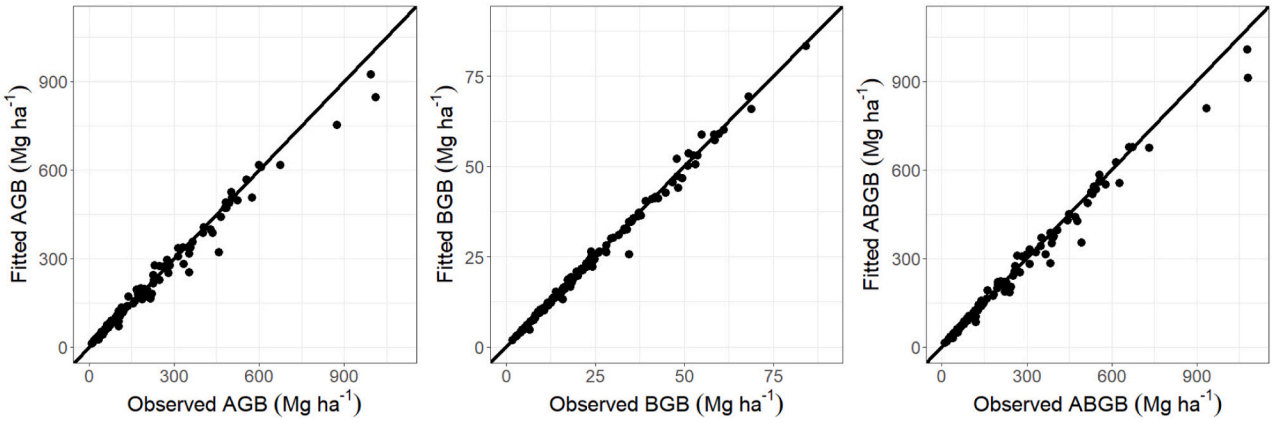

DLAMs 7: 3 predictive covariates*: G, V, T*

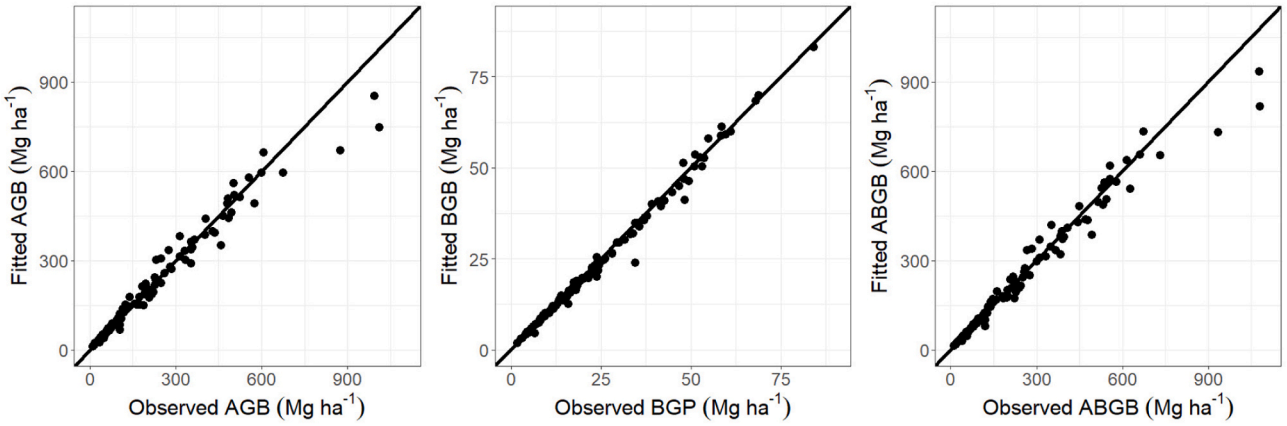

DLAMs 8: 2 predictive covariates: *G, V*

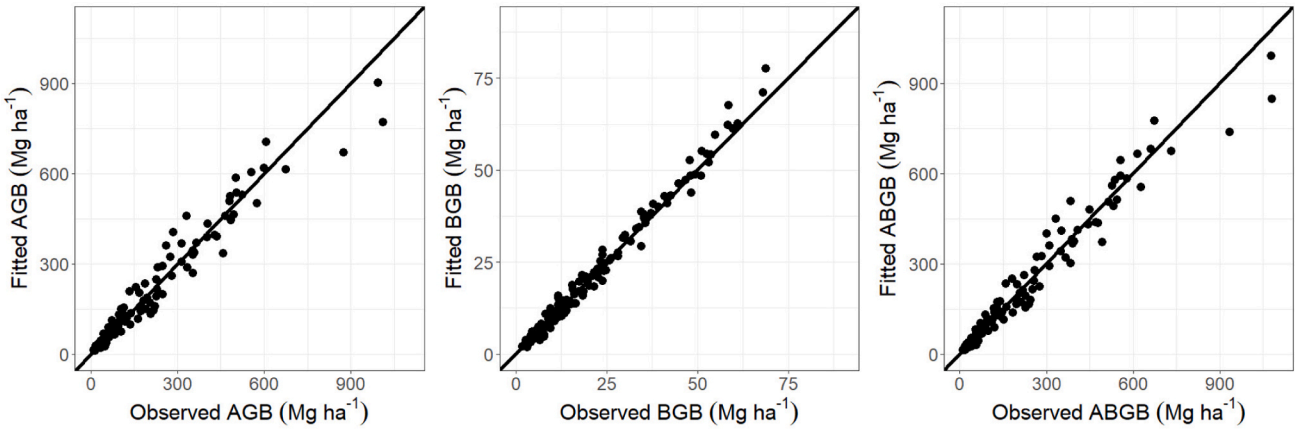

DLAMs 9: 1 predictive variable: *G*

Fig. 7. (*continued*).

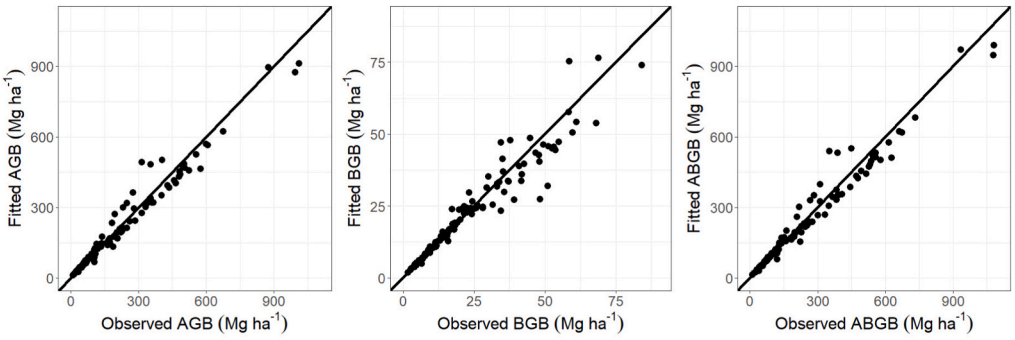

Fig. 7. (*continued*).

4.3. Stand, ecological and environmental factors affect AGB, BGB and ABGB at stand-level in tropical forests

Examining the influence of predictive covariates revealed that forest stand variables, *G*, *V*, *Hg*, and *FT*, have the most significant impact. Environmental and ecological variables such as *T*, *EL*, and *SG* have a pronounced impact on the carbon accumulation of tropical forests. Variations in *T* induced by climate change impact tree growth and biomass accumulation in forests. *T*, which is related to photosynthetic intensity for the accumulation of plant biomass (Law et al. 2002), is an important climatic factor that should be considered for forest biomass (Ma et al. 2023).

On the other hand, in tropical regions, the *EL* factor essentially represents different climatic subzones. It varies and influences climate-related factors such as atmospheric changes subsequently impacting forest biomass accumulation. Additionally, forest soil plays a central role in shaping diverse forest types and species composition, thus influencing the variable capacity for biomass accumulation. These findings are in line with the observations of Pan et al. (2013), highlighting that forest biomass is a complex characteristic influenced by factors such as distribution, structure, and ecological processes within the forest ecosystem. Additionally, the dynamics of forest biomass are influenced by topographic factors (Salinas-Melgoza et al. 2018), such as altitude and climate conditions, with *T* being a particularly significant variable in this regard (Qian et al. 2021). The findings of this study align with the observations made by Balima et al. (2021), which highlight that forest stand variables (specifically, *G* and *V* variables in this study) have a more significant influence on the variation of forest biomass carbon sequestration compared to climatic factors (such as *T* factor in this study) (Fig. 5).

The selection of the best DLAMs (DLAMs 1) involved the inclusion of the optimal seven predictive covariates: *G*, *V*, *T*, *EL*, *FT*, *Hg*, and *SG*, as shown in Table 10. This choice was consistent with the result of the FAMD analysis (Fig. 5), which identified these predictors as having the highest contributions to the variations of the response variables, namely stand-level *AGB*, *BGB*, and *ABGB*.

4.4. The variability of stand-level AGB and BGB in tropical forests

According to IPCC (2003), the average stand-level *AGB* of tropical rainforests in Asia is 280 Mg ha^{-1}, spanning from 120 to 680 Mg ha^{-1}. Specifically, this *AGB* varies in Vietnam from 11 Mg ha^{-1} to 917 Mg ha^{-1} (Table 11), averaging 201 Mg ha^{-1} (Table 1). These figures suggest that natural tropical rainforests in Vietnam have undergone varying degrees of disturbance, with certain regions showing significantly reduced biomass stocks. However, it is worth noting that there are also areas in Vietnam where forests remain well-preserved, boasting biomass stocks exceeding 900 Mg ha^{-1}. This surpasses the maximum value provided by the IPCC (2003), which is 680 Mg ha^{-1}, underscoring the existence of forested regions with exceptionally high biomass stocks.

In Costa Rica, secondary tropical forests also display notable variability in *AGB*, spanning from 1.7 to 409 Mg ha^{-1} (Becknell and Powers 2014). While the variability is less pronounced than Vietnam's, the primary cause remains similar mainly attributed to historical disturbances (Becknell and Powers 2014) or land use factors (Yang et al. 2014). However, in Costa Rica, sustainably managed production forests demonstrate an average *AGB* of 329 Mg ha^{-1}, surpassing that of primary forests (296 Mg ha^{-1}) (Vila et al. 2021). Meanwhile, Colombia's tropical rainforests boast the highest *AGB* sequestration, with a significant stock of 542 Mg ha^{-1} (Calderon-Balcazar et al. 2023). These *AGB* values notably exceed those observed in disturbed forests in Vietnam (201 Mg ha^{-1}).

In the tropical lowlands of Sumatra, Indonesia, the combined *AGB* and *BGB* average 384 Mg ha^{-1} (Kotowska et al. 2015). In contrast, the biomass sequestration in these components (*ABGB*) within the tropical forests of Vietnam varies widely, ranging from 13 Mg ha^{-1} to 994 Mg ha^{-1} (Table 11), with an average of 225 Mg ha^{-1} (Table 1). This comparison highlights significant variability in the stand-level *AGB* and *BGB* of Vietnamese forests, which, on average, is lower than that of forested regions in Southeast Asia, such as Indonesia. According to Kotowska et al. (2015), *AGB* and *BGB* in monoculture rubber and oil palm plantations were reported to be 78 Mg ha^{-1} and 50 Mg ha^{-1}, respectively. Consequently, converting natural tropical forests into monoculture rubber plantations, a trend observed in developing tropical countries over recent decades, leads to emissions of approximately 254 Mg ha^{-1} in CO_{2e} in Vietnam and Indonesia.

Carbon sequestration in both stand-level *AGB* and *BGB* ranges from 6.0 Mg ha^{-1} to 467.0 Mg ha^{-1} in various disturbed forest statuses in Vietnam (Table 11). The average carbon sequestration is estimated to be 105.8 Mg ha^{-1}, calculated using an averaged *ABGB* of 225 Mg ha^{-1} (Table 1) and a default carbon fraction (CF) of 0.47 (IPCC 2006). Conversely, Karmakar et al. (2020) disclosed that the average carbon accumulation in these pools within tropical degraded DDF in India, which have undergone recovery over three decades, amounts to 18.4 Mg ha^{-1}. In contrast, moist central African forests exhibited a total carbon accumulation of 208.1 Mg ha^{-1} in the *AGB* and *BGB* (Ekoungoulou et al. 2015), while a semi-arid forest ecosystem of India displayed 63.5 Mg ha^{-1} (Meena et al. 2019).

This emphasizes the considerable diversity in carbon accumulation within disturbed tropical forests in Vietnam, which, on average, surpasses that of degraded natural forests and semi-arid forests in neighboring countries but falls short of tropical African forests. Tropical natural forests in Vietnam are typically managed for multiple purposes, and it is ideal to pursue these objectives simultaneously. Carbon sequestration and storage optimization are critical forest management goals, particularly given climate change. Hence, it is imperative to

Table 11
Simultaneous predictions of stand-level *AGB*, *BGB*, *ABGB*, Carbon, and CO_2 equivalent (CO_2e) by stand volume *V* classes using DLAMs 10.

ID	*V* (m^3 ha^{-1})	*AGB* (Mg ha^{-1})	*BGB* (Mg ha^{-1})	*ABGB* (Mg ha^{-1})	Carbon (Mg ha^{-1})	CO_2e (Mg ha^{-1})
1	10	10.9	1.8	12.8	6.0	22.0
2	30	28.6	5.3	33.9	15.9	58.5
3	50	45.5	8.4	53.9	25.3	93.0
4	70	61.5	11.7	73.2	34.4	126.2
5	90	76.9	14.8	91.8	43.1	158.3
6	110	94.0	17.7	111.6	52.5	192.6
7	130	111.2	20.6	131.8	61.9	227.3
8	150	131.4	23.3	154.8	72.7	266.9
9	170	155.9	24.1	179.9	84.6	310.4
10	190	178.8	24.1	202.8	95.3	349.8
11	210	194.6	24.0	218.7	102.8	377.2
12	230	210.4	25.1	235.5	110.7	406.1
13	250	226.2	26.2	252.4	118.6	435.4
14	270	242.2	27.3	269.5	126.7	464.8
15	290	258.2	28.5	286.7	134.8	494.6
16	310	274.4	29.8	304.2	143.0	524.7
17	330	291.0	31.1	322.1	151.4	555.6
18	350	308.0	32.5	340.5	160.0	587.3
19	370	325.1	33.9	359.0	168.8	619.3
20	390	342.2	35.4	377.6	177.5	651.3
21	410	359.4	36.8	396.1	186.2	683.3
22	430	376.5	38.2	414.7	194.9	715.3
23	450	393.6	39.7	433.3	203.6	747.3
24	470	410.7	41.1	451.8	212.3	779.3
25	490	427.8	42.5	470.4	221.1	811.3
26	510	445.0	43.9	488.9	229.8	843.3
27	530	462.1	45.4	507.5	238.5	875.3
28	550	479.2	46.8	526.0	247.2	907.3
29	570	496.3	48.2	544.6	255.9	939.3
30	590	513.4	49.7	563.1	264.7	971.3
31	610	530.6	51.1	581.7	273.4	1003.3
32	630	547.7	52.5	600.2	282.1	1035.3
33	650	565.0	53.9	618.8	290.8	1067.4
34	670	582.5	55.0	637.6	299.7	1099.7
35	690	600.1	56.2	656.3	308.5	1132.0
36	710	617.7	57.3	675.0	317.3	1164.4
37	730	635.3	58.4	693.8	326.1	1196.7
38	750	652.9	59.6	712.5	334.9	1229.0
39	770	670.5	60.7	731.2	343.7	1261.3
40	790	688.1	61.9	750.0	352.5	1293.6
41	810	705.7	63.0	768.7	361.3	1326.0
42	830	723.3	64.2	787.5	370.1	1358.3
43	850	740.9	65.3	806.2	378.9	1390.6
44	870	758.5	66.5	824.9	387.7	1422.9
45	890	776.1	67.6	843.7	396.5	1455.2
46	910	793.6	68.7	862.4	405.3	1487.5
47	930	811.2	69.9	881.1	414.1	1519.9
48	950	828.8	71.0	899.9	422.9	1552.2
49	970	846.4	72.2	918.6	431.7	1584.5
50	990	864.0	73.3	937.3	440.5	1616.8
51	1010	881.6	74.5	956.1	449.4	1649.1
52	1030	899.2	75.6	974.8	458.2	1681.5
53	1050	916.8	76.8	993.5	467.0	1713.8

Note: *AGB* is the aboveground biomass, *BGB* is the belowground biomass, and *ABGB* is the above- and belowground biomass at stand-level. Carbon is the carbon sequestration in both above- and belowground biomass = 0.47 × *ABGB*, where 0.47 is the default carbon fraction (CF) of IPCC (2006). CO_2e is the equivalent CO_2 absorption in both above- and belowground carbon pools = 3.67 × Carbon.

consider the effects of forest harvesting and disturbances on carbon stock and dynamics to formulate projections for potential carbon sequestration and storage.

4.5. Application of DLAMs

Based on the results of the cross-validations comparisons, the DLAMs are recommended as an alternative to conventional statistical nonlinear regressions such as WNSUR and MARS, respectively, for simultaneously predicting *AGB*, *BGB* and their sum *ABGB* at the stand-level in tropical forests. Furthermore, using DLAMs to predict biomass carbon in tropical mixed-species forests at the stand-level can yield cost savings when compared to tree-level biomass equations, primarily because there is no requirement to identify tree species or species-specific *wd* variables.

One of the best-saved results from the DLAMs 1–10 can be selected for practical applications. A Python script can be executed to import the chosen DLAMs, and the newly provided dataset file contains the values of the predictive covariates used in the selected DLAMs. This will allow for predicting *AGB*, *BGB*, and *ABGB* simultaneously while ensuring additivity at the stand-level of tropical forests.

The selection of which DLAMs to use should depend on the availability of resources for data collection of predictive covariates and cost-effectiveness. However, the best DLAMs, DLAMs 1, with optimal seven predictive variables (*G*, *V*, *T*, *EL*, *FT*, *Hg*, and *SG*), is recommended, as it has demonstrated the highest level of reliability and the lowest prediction errors when simultaneously predicting stand-level *AGB*, *BGB*, and *ABGB*. Furthermore, since the national forest database mainly includes the attribute of stand volume *V*, DLAMs 10 can be selected to convert attribute *V* to stand-level biomass. On the other hand, in certain areas where local community participation is involved in forest carbon measurement and monitoring, and the observed attribute of the forest is simplified to include only one variable, *d*, it is recommended to utilize DLAMs 9 with only the *G* predictor (derived from the *d* measurement). However, using DLAMs 9–10 with a single predictor variable, *G* or *V*, will generally result in lower reliability than the best DLAMs 1 model. Table 10 provides the goodness-of-fit and error metrics for these modeling systems.

DLAMs can be applied to small areas, such as a forest block spanning a few hectares, or to larger ecological regions, territories, or even countries. A few purposive sample plots can be established for the forest block to measure and collect the predictor variables. On the other hand, when DLAMs are applied to larger areas, it is necessary to establish a systematic sample plot system to measure and collect predictor variables tailored to the specific requirements of the selected DLAMs. The sample plots should be stratified based on forest type and forest status, and the number of plots should be sufficient to ensure the desired level of precision as defined by IPCC (2003).

When applying the best DLAMs 1 with the optimal seven predictor variables (*G*, *V*, *T*, *EL*, *FT*, *Hg*, and *SG*), the variables to be measured in each sample plot are *d* and *h*. *d* is measured to derive *G*, while both *d* and *h* are used to derive *V* and *Hg* is calculated based on *Dg*. The factor *T* can be extracted based on the coordinates of each sample plot from a raster file with a spatial resolution of 30 s (~1 km), which contains the mean annual temperature (Fick and Hijmans 2017). The *EL* factor is recorded in each plot and the *SG* predictor should be extracted from the soil map of FAO-UNESCO (2005). However, collecting data from the sample plot is unnecessary if the DLAMs 10 is applied with a single variable, *V*. Instead, existing and updated forest databases at the regional or national level, with the attribute *V* categorized by forest type and forest status, can be utilized. If the DLAMs 9 is applied with a single variable, *G*, only the measurement of variable *d* is required for each sample plot. A user-friendly system, including an executable package and a user guide, is available for download to facilitate efficient and practical applications at https://baohuy-frem.org/deep-learning-for-forest-biomass-prediction/.

The development and application of stand-level biomass models greatly contribute to studying tropical forest ecosystem productivity and carbon cycles at multiple scales (Xin et al. 2023). Furthermore, using stand-level biomass carbon models reduces dependence on specialized resources compared to implementing tree-level allometric models. Specifically, the utilization of the advanced DLAMs 1 modeling system at the stand-level eliminates the need for species identification, which is otherwise required for converting into tree wood density values used in tree-level biomass equations (Huy et al. 2016a, 2016b; Kralicek et al. 2017) (Table 2) for tropical mixed-species forests. However, it should be noted that using the DLAMs at the stand-level as a supplement can

Table 12
Comparison of cross-validation results for simultaneously predicting stand-level *AGB*, *BGB* and *ABGB* using different three approaches: Deep Learning Additive Models (DLAMs), Multivariate Adaptive Regression Splines (MARS) and Weighted Non-Linear Seemingly Unrelated Regression (WNSUR) modeling systems, with their optimal predictive covariates.

ID	Methods	Optimal predictors	Modeling systems	FI	Bias (%)	RMSE (Mg ha^{-1})	MAPE (%)
1	DLAMs	7 predictive covariates: *G*, *V*, *T*, *EL*, *FT*, *Hg*, *SG*	The best modeling system (DLAMs 1)				
			The best model of *AGB*	0.986	−1.57	22.8	6.29
			The best model of *BGB*	0.989	−0.81	1.6	4.27
			The best model of $ABGB = AGB + BGB$	0.987	−1.38	16.2	5.28
2	MARS	5 predictive covariates: *G*, *V*, *T*, *EL*, *Hg*	The best modeling system				
			The best model of *AGB*	0.981	0.73	28.1	10.61
			The best model of *BGB*	0.956	−7.11	3.6	15.91
			The best model of $ABGB = AGB + BGB$	0.982	−0.36	29.6	9.41
3	WNSUR	6 predictive covariates: *G*, *V*, *T*, *EL*, *Hg*, *SG*	The best modeling system				
			$AGB = a_1 V^{b11} Hg^{b12} \exp(e_{11} / 100(T - 22.9) + (e_{12} / 1000)(EL - 613) + e_{14}(SG - 1.7))$	0.986	2.88	28.3	9.17
			$BGB = a_2 G^{b21} \exp(e_{21} / 100(T - 22.9) + (e_{22} / 1000)(EL - 613))$	0.886	−3.30	4.2	18.31
			$ABGB = AGB + BGB$	0.989	1.99	29.1	7.71

Note: *AGB* is the aboveground biomass (Mg ha^{-1}), *BGB* is the belowground biomass (Mg ha^{-1}), and *ABGB* is the above- and belowground biomass (Mg ha^{-1}) at stand-level. *G* (m^2 ha^{-1}): stand basal area per hectare, *V* (m^3 ha^{-1}): stand volume per hectare, *T* (°C year-averaged): mean annual temperature, *EL*: elevation (m), *FT*: forest type, DDF: Dry Dipterocarp Forest, EBLF: Evergreen Broadleaf Forest, *Hg* (m): the height of the tree with a *Dg* (the quadratic mean diameter at breast height), *SG*: soil group, FA: Ferric Acrisols, OA: Orthic Acrisols, RF: Rhodic Ferrasols. All statistics were calculated using cross-validation, 70 % randomly split dataset for training models, and 30 % randomly split dataset for validating; finally, all statistics and error metrics averaged over 10 realizations; the optimal DLAMs was selected based on its performance across 10 cross-validation folds, and its statistics and error metrics were computed to assess its effectiveness in the validation process.

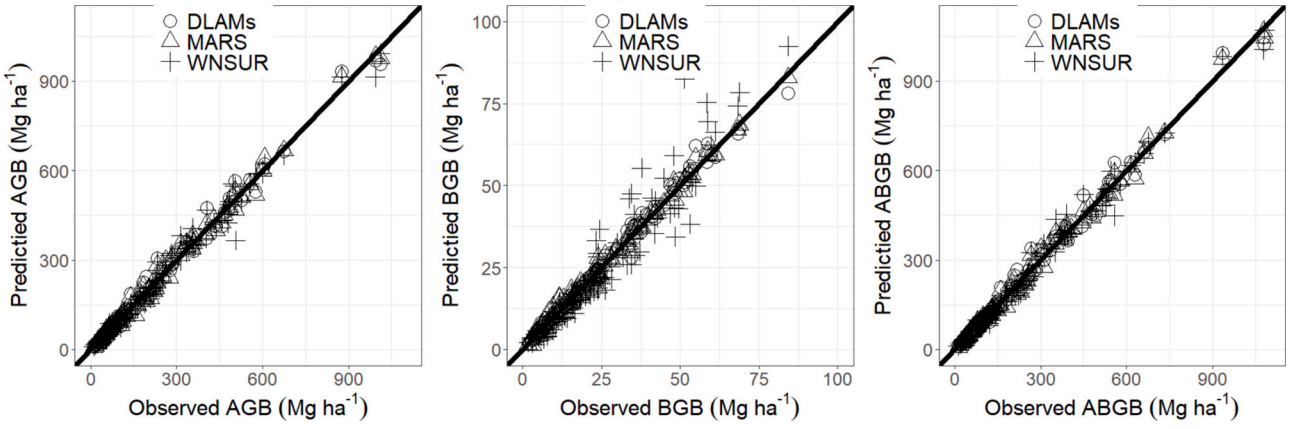

Fig. 8. Comparison of predicted vs. observed biomass components of *AGB* (aboveground biomass), *BGB* (belowground biomass), and *ABGB* (above- and belowground biomass) at stand-level by the Deep Learning Additive Models (DLAMs) with its seven optimal predictive covariates (*G*, *V*, *T*, *EL*, *FT*, *Hg*, and *SG*), the Multivariate Adaptive Regression Splines (MARS) modeling system with its five optimal predictive covariates (*G*, *V*, *T*, *EL*, and *Hg*), and the Weighted Non-Linear Seemingly Unrelated Regression (WNSUR) modeling system with its six optimal predictive covariates (*G*, *V*, *T*, *EL*, *Hg*, and *SG*).
Note: *G* (m^2 ha^{-1}): stand basal area per hectare; *V* (m^3 ha^{-1}): stand volume per hectare; *T* (°C year-averaged): mean annual temperature; *EL*: elevation (m); *FT*: forest type, DDF: Dry Dipterocarp Forest, EBLF: Evergreen Broadleaf Forest; *Hg* (m): the height of the tree with a *Dg* (the quadratic mean diameter at breast height); *SG*: soil group, FA: Ferric Acrisols, OA: Orthic Acrisols, RF: Rhodic Ferrasols.

slightly increase the error compared to using only the WNSUR or, MARS or DL modeling systems at the tree-level to predict tree *AGB*, *BGB*, and their total simultaneously.

5. Conclusions

This study offered compelling evidence that the use of innovative DLAMs substantially enhanced the reliability of simultaneously predicting *AGB*, *BGB*, and their sum *ABGB* while ensuring additivity at stand-level in tropical forests, surpassing conventional simultaneous modeling systems that employed statistical nonlinear simultaneous regressions, such as WNSUR and MARS, respectively. Furthermore, using DLAMs to predict tropical mixed-species forest biomass carbon at the stand-level will reduce resource costs compared to tree-level biomass equations because there is no requirement to identify tree species or species-specific *wd* predictive variables.

DLAMs 1 emerged as the best modeling system for simultaneously predicting stand-level *AGB*, *BGB*, and *ABGB*, and integrating seven optimal predictive covariates (*G*, *V*, *T*, *EL*, *FT*, *Hg*, and *SG*). It demonstrated the highest level of reliability and the lowest prediction errors, unequivocally affirming its superior performance. The best DLAMs (DLAMs 1) achieved FIs of 0.986, 0.989 and 0.987, along with MAPEs of 6.3 %, 4.3 % and 5.3 % for the simultaneous predictions of stand-level *AGB*, *BGB* and *ABGB*, respectively.

We recommend using DLAMs 10 to simplify the process to convert the *V* attribute from the updated national forest database into biomass carbon pools. On the other hand, when the local community participates in forest carbon measurement and monitoring, and only the simple tree variable *d* is measured, it is advised to utilize DLAMs 9 with only the *G* predictor. However, using DLAMs 9 and 10 will generally result in lower reliability.

In the two biomass carbon pools, aboveground and belowground, in Vietnam's tropical forest statuses, the biomass, carbon sequestration, and CO_2e absorption exhibit variations, ranging from 13 to 994 Mg

ha^{-1}, from 6 to 467 Mg ha^{-1}, and from 22 to 1714 Mg ha^{-1}, respectively.

To align with the specific observed dataset and account for the varying relationships among surveyed variables, conducting experiments in designing the architecture, selecting algorithms, and tuning hyperparameters for MODNNs is crucial. The appropriate selection of these components significantly enhances the reliability of predictions for the multi-output variables within DLAMs.

CRediT authorship contribution statement

Bao Huy: Writing – review & editing, Writing – original draft, Visualization, Validation, Software, Resources, Methodology, Investigation, Funding acquisition, Formal analysis, Data curation, Conceptualization. **Krishna P. Poudel:** Writing – review & editing, Validation, Methodology. **Hailemariam Temesgen:** Writing – review & editing, Validation, Supervision, Methodology. **Christian Salas-Eljatib:** Writing – review & editing, Validation, Methodology. **Nguyen Quy Truong:** Writing – original draft, Software, Methodology. **Nguyen Quy Khiem:** Writing – original draft, Project administration, Investigation, Formal analysis, Data curation.

Funding sources

This research did not receive any specific grant from funding agencies in the public, commercial, or not-for-profit sectors.

Declaration of competing interest

The authors declare that they have no known competing financial interests or personal relationships that could have appeared to influence the work reported in this paper.

Acknowledgments

The original raw dataset was collected through studies conducted by the Forest Resources and Environment Management Consultancy (FREM) and the UN-REDD program in Vietnam.

Data availability

Data will be made available on request.

References

Akaike, H., 1973. Information theory as an extension of the maximum likelihood principle. In: Petrov, B.N., Csaki, F.E. (Eds.), 2nd Int Symp on Information Theory. Akademiai Kiado, Budapest, pp. 267–281.

Arjasakusuma, S., Kusuma, S.S., Phinn, S., 2020. Evaluating variable selection and machine learning algorithms for estimating forest heights by combining Lidar and hyperspectral data. ISPRS Int. J. Geo Inf. 9, 507. https://doi.org/10.3390/ijgi9090507.

Bai, Y., 2022. RELU-function and derived function review. In: SHS Web of Conferences, vol. 144, 02006. STEHE, pp. 2–5. https://doi.org/10.1051/shsconf/202214402006.

Balima, L.H., Kouamec, F.N., Bayen, P., Ganame, M., Nacoulma, B.M.I., Thiombiano, A., Soro, D., 2021. Influence of climate and forest attributes on aboveground carbon storage in Burkina Faso, West Africa. Environ. Chall. 4 (2021), 100123. https://doi.org/10.1016/j.envc.2021.100123.

Becknell, J.M., Powers, J.S., 2014. Stand age and soils as drivers of plant functional traits and aboveground biomass in secondary tropical dry forest. Can. J. For. Res. 44, 604–613. https://doi.org/10.1139/cjfr-2013-0331.

Calderon-Balcazar, A., Cardenas, C.D., Diaz-Vasco, O., Fandino, E., Marquez, T., Pizano, C., 2023. Biomass and carbon stocks of four vegetation types in the Llanos Orientales of Colombia (Mapiripan, Meta). Trees For. People 12 (2023), 100380. https://doi.org/10.1016/j.tfp.2023.100380.

Chollet, F., 2018. Deep Learning With Python. Manning, Shelter Island, NY, USA, 386 pp.

Ekoungoulou, R., Niu, S., Loumeto, J.J., Ifo, S.A., Bocko, Y.E., Mikieleko, F.E.K., Guiekisse, E.D.M., Senou, H., Liu, X., 2015. Evaluating the carbon stock in above- and belowground biomass in a moist central African forest. Appl. Ecol. Environ. Sci. 3 (2), 51–59. https://doi.org/10.12691/aees-3-2-4.

Ercanli, I., 2020. Innovative deep learning artificial intelligence applications for predicting relationships between individual tree height and diameter at breast height. For. Ecosyst. 7, 12. https://doi.org/10.1186/s40663-020-00226-3.

FAO-UNESCO, 2005. Soil Map of the World, Digitized by ESRI. Soil Climate Map. USDA-NRCS, Soil Science Division, World Soil Resources, Washington D.C.

Fick, S.E., Hijmans, R.J., 2017. WorldClim 2: new 1 km spatial resolution climate surfaces for global land areas. Int. J. Climatol. 37 (12), 4302–4315.

Filippi, A.M., Guneralp, I., Randall, J., 2014. Hyperspectral remote sensing of aboveground biomass on a river meander bend using multivariate adaptive regression splines and stochastic gradient boosting. Remote Sens. Lett. 5 (5), 432–441. https://doi.org/10.1080/2150704X.2014.915070.

Friedman, J.H., 1991. Multivariate adaptive regression splines. Ann. Stat. 19 (1), 1–141. https://doi.org/10.1214/aos/1176347963.

Friedman, J.H., 1993. Estimating functions of mixed ordinal and categorical variables using adaptive splines. In: Morgenthaler, Stephan, Ronchetti, Elvezio, Stahel, Werner (Eds.), New Directions in Statistical Data Analysis and Robustness. Birkhauser.

Friedman, J.H., Silverman, B.W., 1989. Flexible parsimonious smoothing and additive modeling. Technometrics 31 (1), 3–21. http://links.jstor.org/sici?sici=0040-1706%28198902%2931%3A1%3C3%3AFPSAAM%3E2.0.CO%3B2-Z.

Genc, S.K., Diamantopoulou, M.J., Ozcelik, R., 2023. Tree biomass modeling based on the exploration of regression and artificial neural networks approaches. Forests 14 (12), 2429. https://doi.org/10.3390/f14122429.

He, X., Lei, X., Liu, D., Lei, Y., 2023. Developing machine learning models with multiple environmental data to predict stand biomass in natural coniferous-broad leaved mixed forests in Jilin Province of China. Comput. Electron. Agric. 212 (2023), 108162. https://doi.org/10.1016/j.compag.2023.108162.

Huang, H., Ji, X., Xia, F., Huang, S., Shang, X., Chen, H., Zhang, M., Dahlgren, R.A., Mei, K., 2019. Multivariate adaptive regression splines for estimating riverine constituent concentrations. Hydrol. Process. 34 (5), 1–15. https://doi.org/10.1002/hyp.13669.

Huy, B., Kralicek, K., Poudel, K.P., Phương, V.T., Khoa, P.V., Hung, N.D., Temesgen, H., 2016a. Allometric equations for estimating tree aboveground biomass in evergreen broadleaf forests of Viet Nam. For. Ecol. Manag. 382 (2016), 193–205. https://doi.org/10.1016/j.foreco.2016.10.021.

Huy, B., Poudel, K.P., Kralicek, K., Hung, N.D., Khoa, P.V., Phuong, V.T., Temesgen, H., 2016b. Allometric equations for estimating tree aboveground biomass in tropical dipterocarp forests of Viet Nam. Forests 7 (180), 1–19. https://doi.org/10.3390/f7080180. http://www.mdpi.com/1999-4907/7/8/180.

Huy, B., Tinh, N.T., Poudel, K.P., Frank, B.M., Temesgen, H., 2019. Taxon-specific modeling systems for improving reliability of tree aboveground biomass and its components estimates in tropical dry dipterocarp forests. For. Ecol. Manag. 437 (2019), 156–174. https://doi.org/10.1016/j.foreco.2019.01.038.

Huy, B., Truong, N.Q., Khiem, N.Q., Poudel, K.P., Temesgen, H., 2022a. Stand growth modeling system for planted teak (*Tectona grandis* L.f.) in tropical highlands. Trees For. People 9 (2022), 100308. https://doi.org/10.1016/j.tfp.2022.100308.

Huy, B., Truong, N.Q., Khiem, N.Q., Poudel, K.P., Temesgen, H., 2022b. Deep learning models for improved reliability of tree aboveground biomass prediction in the tropical evergreen broadleaf forests. For. Ecol. Manage. 508 (2022), 1–13. https://doi.org/10.1016/j.foreco.2022.120031, 120031.

Huy, B., Khiem, N.Q., Truong, N.Q., Poudel, K.P., Temesgen, H., 2023. Additive modeling systems to simultaneously predict aboveground biomass and carbon for *Litsea glutinosa* of agroforestry model in tropical highlands. For. Syst. 32 (1), e006. https://doi.org/10.5424/fs/2023321-19780.

Huy, B., Truong, N.Q., Poudel, K.P., Temesgen, H., Khiem, N.Q., 2024. Multi-output deep learning models for enhanced reliability of simultaneous tree above- and belowground biomass predictions in tropical forests of Vietnam. Comput. Electron. Agric. 222 (2024), 109080. https://doi.org/10.1016/j.compag.2024.109080.

IPCC, 2003. Good Practice Guidance for Land Use, Land-Use Change and Forestry. IPCC National Greenhouse Gas Inventories Programme, Hayama, Japan, 295 pp.

IPCC, 2006. IPCC guidelines for national greenhouse gas inventories. In: Eggleston, H.S., Buendia, L., Miwa, K., Ngara, T., Tanabe, K. (Eds.), Prepared by the National Greenhouse Gas Inventories Programme. IGES, Japan.

Karmakar, S., Pradhan, B.S., Bhardwaj, A., Pavan, B.K., Chaturvedi, R., Chaudhry, P., 2020. Assessment of above- and belowground carbon pools in a tropical dry deciduous forest ecosystem of Bhopal, India. Chin. J. Urban Environ. Stud. 8 (4), 2050021. https://doi.org/10.1142/S2345748120500219.

Keras, 2022. K Keras–Simple. Flexible. Powerful. https://keras.io/.

Koc, E.K., Bozdogan, H., 2015. Model selection in multivariate adaptive regression splines (MARS) using information complexity as the fitness function. Mach. Learn. 2015 (101), 35–58. https://doi.org/10.1007/s10994-014-5440-5.

Kotowska, M.M., Leuschner, C., Triadiati, T., Meriem, S., Hertel, D., 2015. Quantifying above- and belowground biomass carbon loss with forest conversion in tropical lowlands of Sumatra (Indonesia). Glob. Chang. Biol. 21 (10). https://doi.org/10.1111/gcb.12979.

Kralicek, K., Huy, B., Poudel, K.P., Temesgen, H., Salas, C., 2017. Simultaneous estimation of above- and belowground biomass in tropical forests of Viet Nam. For. Ecol. Manag. 390 (2017), 147–156. http://www.sciencedirect.com/science/article/pii/S0378112716307411.

Laurin, G.V., Puletti, N., Chen, Q., Corona, P., Papale, D., Valentini, R., 2016. Above ground biomass and tree species richness estimation with airborne lidar in tropical Ghana forests. Int. J. Appl. Earth Obs. Geoinf. 52 (2016), 371–379. https://doi.org/10.1016/j.jag.2016.07.008.

Law, B.E., Falge, E., Gu, L., Baldocchi, D.D., Bakwin, P., Berbigier, P., Davis, K., Dolman, A.J., Falk, M., Fuentes, J.D., Goldstein, A., Granier, A., Grelle, A., Hollinger, D., Janssens, I.A., Jarvis, P., Jensen, N.O., Katul, G., Mahli, K., Matteucci, G., Meyers, T., Monson, R., Munger, W., Oechel, W., Olson, R.,

Pilegaard, K., Paw, U.K.T., Thorgeirsson, H., Valentini, R., Verma, Shashi, Vesala, T., Wilson, K., Wofsy, S., 2002. Environmental controls over carbon dioxide and water vapor exchange of terrestrial vegetation. Pap. Nat. Resour. 65. https://digitalcommons.unl.edu/natrespapers/65.

Lê, S., Josse, J., Husson, F., 2008. FactoMineR: an R package for multivariate analysis. J. Stat. Softw. 25 (1), 1–18. https://doi.org/10.18637/jss.v025.i01.

LeCun, Y., Bengio, Y., Hinton, G., 2015. Deep learning. Nature 521 (2015), 436–444. https://doi.org/10.1038/nature14539.

Lei, X., 2019. Applications of machine learning algorithms in forest growth and yield prediction. J. Beijing For. Univ. 41 (12), 23–36. https://doi.org/10.12171/j.1000-1522.20190356.

Lindstrom, M.J., Bates, D.M., 1990. Nonlinear mixed effects models for repeated measures data. Biometrics 46, 673–687.

Ma, Y., Eziz, A., Halik, U., Abliz, A., Kurban, A., 2023. Precipitation and temperature influence the relationship between stand structural characteristics and aboveground biomass of forests — a meta-analysis. Forests 2023 (14), 896. https://doi.org/10.3390/f14050896.

McKinney, W., Pandas Development Team, 2022. pandas: Powerful Python Data Analysis Toolkit. Release 1.4.4. Pandas, 3743 pp.

Meena, A., Bidalia, A., Hanief, M., Dinakaran, J., Rao, K.S., 2019. Assessment of above- and belowground carbon pools in a semi-arid forest ecosystem of Delhi, India. Ecol. Process. 8, 8. https://doi.org/10.1186/s13717-019-0163-y.

Milborrow, S., 2021. Notes on the earth package. Available at http://www.milbo.org/doc/earth-notes.pdf. access on July 13, 2023.

Milborrow, S., 2023. Package 'earth'. Repository CRAN. Available at http://www.milbo.users.sonic.net/earth/. access on July 13, 2023.

Naser, A.H., Badr, A.H., Henedy, S.N., Ostrowski, K.A., Imran, H., 2022. Application of Multivariate Adaptive Regression Splines (MARS) approach in prediction of compressive strength of eco-friendly concrete. Case Stud. Construct. Mater. 17 (2022), e01262. https://doi.org/10.1016/j.cscm.2022.e01262.

Ogana, F.N., Ercanli, I., 2021. Modeling height-diameter relationships in complex tropical rain forest ecosystems using deep learning algorithm. J. For. Res. https://doi.org/10.1007/s11676-021-01373-1.

Ozdemir, S., Kucuksille, E.U., Gulsoy, S., Senturk, O., Negiz, M.G., Suel, H., Mert, A., Ozkan, K., 2022. Modeling of species distributions with deep learning method. In: 6th International Conference on Computational Mathematics and Engineering Sciences, 20–22 May 2022, Ordu, Turkey, pp. 180–190.

Pan, Y., Birdsey, R.A., Phillips, O.L., Jackson, R.B., 2013. The structure, distribution, and biomass of the world's forests. Annu. Rev. Ecol. Evol. Syst. 44, 593–622. https://doi.org/10.1146/annurev-ecolsys-110512-135914.

Parresol, B.R., 2001. Additivity of nonlinear biomass equations. Can. J. For. Res. 31 (5), 865–878.

Poudel, K.P., Temesgen, H., 2016. Methods for estimating aboveground biomass and its components for Douglas-fir and lodgepole pine trees. Can. J. For. Res. 46, 77–87. https://doi.org/10.1139/cjfr-2015-0256.

Pravalie, R., Niculita, M., Rosca, B., Patriche, C., Dumitrascu, M., Marin, G., Nita, I.A., Bandoc, G., Birsan, M.V., 2023. Modelling forest biomass dynamics in relation to climate change in Romania using complex data and machine learning algorithms. Stoch. Environ. Res. Risk A 37, 1669–1695. https://doi.org/10.1007/s00477-022-02359-z.

Python, 2022. Python packaging user guide. https://packaging.python.org/.

Qian, C., Qiang, H., Zhang, G., Li, M., 2021. Long-term changes of forest biomass and its driving factors in karst area, Guizhou, China. Int. J. Distrib. Sensor Netw. 17 (8). https://doi.org/10.1177/15501477211039137.

Qin, Y., Wu, B., Lei, X., Feng, L., 2023. Prediction of tree crown width in natural mixed forests using deep learning algorithm. For. Ecosyst. https://doi.org/10.1016/j.fecs.2023.100109.

R Core Team, 2023. A Language and Environment for Statistical Computing. R Foundation for Statistical Computing, Vienna, Austria. http://www.r-project.org/index.html.

Salinas-Melgoza, M.A., Skutsch, M., Lovett, J.C., 2018. Predicting aboveground forest biomass with topographic variables in human-impacted tropical dry forest landscapes. Ecosphere 9 (1), e02063. https://doi.org/10.1002/ecs2.2063.

Sarker, I.H., 2021. Deep learning: a comprehensive overview on techniques, taxonomy, applications and research directions. SN Comput. Sci. 2 (8), 420. https://doi.org/10.1007/s42979-021-00815-1. Epub 2021 Aug 18. PMID: 34426802; PMCID: PMC8372231.

SAS Institute Inc., 2014. SAS/ETS® 13.2 User's Guide. Chapter 19: The MODEL Procedure. SAS Institute Inc., Cary, NC, pp. 1067–1373.

Seely, H., Coops, N.C., White, J.C., Montwe, S.D., Winiwarter, L., Ragab, A., 2023. Modelling tree biomass using direct and additive methods with point cloud deep learning in a temperate mixed forest. Sci. Remote Sens. 8 (2023), 100110. https://doi.org/10.1016/j.srs.2023.100110.

TensorFlow, 2023. Create production-grade machine learning models with TensorFlow. https://www.tensorflow.org/. Access date: Jan. 10, 2023.

USAID, 2018. Carbon payment for forest environmental services (C-PFES): a feasibility study identifying opportunities, challenges, and proposed next steps for application of C-PFES in Vietnam. Tech. Rep. 77. https://doi.org/10.13140/RG.2.2.13220.63360.

Vanclay, J.K., 1994. Modelling Forest Growth and Yield: Applications to Mixed Tropical Forests. CAB International.

Vashum, K.T., Jayakumar, S., 2012. Methods to estimate aboveground biomass and carbon stock in natural forests — a review. J. Ecosyst. Ecogr. 2, 116. https://doi.org/10.4172/2157-7625.1000116.

Vila, L.M., Ménager, M., Finegan, B., Delgado, D., Casanoves, F., Salas, L.A.A., Castillo, M., Sánchez, L.G.H., Méndez, Y., Toruño, H.S., Solano, G., Mora, P.Z., Bieng, M.A.N., 2021. Aboveground biomass storage potential in primary rain forests managed for timber production in Costa Rica. For. Ecol. Manage. 497 (2021), 119462. ISSN 0378-1127. https://doi.org/10.1016/j.foreco.2021.119462.

Wang, Y., Zhang, W., Gao, R., et al., 2021. Recent advances in the application of deep learning methods to forestry. Wood Sci. Technol. 55 (2021), 1171–1202. https://doi.org/10.1007/s00226-021-01309-2.

Xin, S., Shahzad, M.K., Mahardika, S.B., Wang, W., Jiang, L., 2023. An alternative method for estimation of stand-level biomass for three conifer species in Northeast China. Forests 2023 (14), 1274. https://doi.org/10.3390/f14061274.

Xu, D., Shi, Y., Tsang, I.W., Ong, Y.S., Gong, C., Shen, X., 2020. Survey on multi-output learning. IEEE Trans. Neur. Netw. Learn. Syst. 31 (7), 2409–2429. https://doi.org/10.1109/TNNLS.2019.2945133.

Xu, Q., Lei, X., Zhang, H., 2022. A novel method for approaching the compatibility of tree biomass estimation by multi-task neural networks. For. Ecol. Manag. 508 (2022), 120011.

Yang, J., Xu, R., Cai, Z., Bi, J., Wang, H., 2014. Forest biomass carbon storage. BioResources 9 (1), 357–371.

Yasmirullah, S.D.P., Bambang Widjanarko Otok, B.W., Purnomo, J.D.T., Prastyo, D.D., 2021. Modification of multivariate adaptive regression spline (MARS). J. Phys. Conf. Ser. 1863 (2021), 012078. https://doi.org/10.1088/1742-6596/1863/1/012078.

Zanne, A.E., Lopez-Gonzalez, G., Coomes, D.A., Ilic, J., Jansen, S., Lewis, S.L., Miller, R. B., Swenson, N.G., Wiemann, M.C., Chave, J., 2009. Global Wood Density Database. Dryad. Identifier: http://hdl.handle.net/10255/dryad.235.

Zeng, W., Zhang, L., Chen, X., Cheng, Z., Ma, K., Li, Z., 2017. Construction of compatible and additive individual-tree biomass models for *Pinus tabulaeformis* in China. Can. J. For. Res. 47, 467–475. https://doi.org/10.1139/cjfr-2016-0342.

Zeng, W., Zou, W., Chen, X., Yang, X., 2024. A three-level model system of biomass and carbon storage for all forest types in China. Forests 15 (8), 1305. https://doi.org/10.3390/f15081305.

Zhang, F., Wang, X., Guan, J., 2021. A novel multiple-input multiple-output recurrent neural network based on multimodal fusion and spatiotemporal prediction for 0–4 precipitation nowcasting. Atmosphere 2021 (12), 1596. https://doi.org/10.3390/atmos12121596.